nature chemistry

REVIEW ARTICLE

https://doi.org/10.1038/s41557-019-0392-9

Covalent on-surface polymerization

Leonhard Grill[1*] and Stefan Hecht[2,3,4,5*]

With the rapid development of scanning probe microscopy, it has become possible to study polymerization processes on suitable surfaces at the atomic level and in real space. In the two-dimensional confinement of a surface, polymerization reactions can give rise to the formation of unprecedented polymers with unique structures and properties, not accessible in solution. After a little over one decade since the discovery of covalent on-surface polymerization, we give an overview of the field, analyse the crucial aspects and critically reflect on the status quo. Specifically, we provide some general considerations about fundamental mechanisms as well as kinetics and thermodynamics of on-surface polymerization processes. The important role of the surface is detailed in view of its ability to control polymer formation with regard to structure, dimensionality and composition. Furthermore, examples that allow for locally induced polymerization are highlighted. Finally, we provide an analysis of scientific challenges in the field and outline future prospects.

Synthetic chemistry, and in particular catalysis, encompasses both homogeneous and heterogeneous processes. While homogeneous reactions offer the advantage of efficient mixing of substrates, the interface at the phase boundary offers unique advantages in heterogeneous processes: the catalytic activity of the typically solid surface, its anisotropy, chirality and templating effect as well as the facilitated separation/purification. Examples such as the (possibly symmetry breaking) reactions of prebiotic molecules on inorganic mineral surfaces millions of years ago and industrial ammonia synthesis, developed by Haber and Bosch about a century ago, are testament to the power of heterogeneous catalysis and the importance of solid surfaces to enable, facilitate and catalyse specific chemical transformations.

In the context of polymerization, heterogeneous catalysts were the first to be used to produce high-density polyethylene, as pioneered by Ziegler in the early 1950s[1]. The advent of nanoscience and nanotechnology was triggered by the development of scanning tunnelling microscopy (STM) by Binnig, Rohrer and Gerber in the 1980s[2] which, for the first time, enabled researchers to atomically resolve solid surfaces and image individual molecules on them. While investigations of small molecules on metal substrates by STM helped to reveal detailed insight into ammonia synthesis among others[3], studies of polymeric entities suffered from limited sample preparation. Although a large variety of typically sheet-like supramolecular polymers could successfully be prepared by self-assembly of small-molecule building blocks[4,5], covalent polymers were not studied — simply because they could not be evaporated intact due to their high molecular weight (and limited thermal stability).

Inspired by the vision of Drexler's assembler[6], and in particular by the key demonstration of covalent assembly at the single-molecule level using the STM tip by Hla, Rieder and co-workers[7], we serendipitously discovered the in situ formation of covalent polymers directly on the surface after evaporating molecular precursors[8]. The successful formation of a chemical bond is not only visible in microscopy images via the characteristic geometric arrangement — and also well-defined distance — of the linked monomers, but also can be clearly identified via electronic features that are a spectroscopic fingerprint for covalent bonding[8]. Importantly, the monomer building blocks were linked at predetermined (activated) positions, allowing for the rational synthesis of one-dimensional (1D) polymer chains and two-dimensional (2D) polymer networks, and thus providing the basis of what is nowadays referred to as 'on-surface polymerization'[9].

Starting from some key findings about one decade ago[10], this area of research at the interface of matter as well as disciplines has witnessed an enormous development with an ever-increasing number of publications and, even more importantly, many important breakthrough contributions. It is fair to state that 'on-surface polymerization' has developed into a respected modern method of preparing otherwise inaccessible polymer architectures with unique functions, as impressively highlighted by the precision synthesis of graphene nanoribbons (GNRs) by Fasel and Müllen[11,12]. In this Review Article, we highlight the current state of the art in the rapidly growing field of on-surface polymerization from both physical and chemical perspectives. We focus on covalent polymerizations in single molecular layers on solid, atomically defined surfaces, in contrast to, for instance, nanoparticles[13], soft air/liquid interfaces (for example, Langmuir–Blodgett films[14]) or exfoliation of layered systems[15]. Polymers composed of metal–ligand coordination bonds, although used very successfully for the formation of 1D and 2D supramolecular nanostructures[5], are not included.

Polymerizations on planar crystalline surfaces are characterized by two unique features. On the one hand, the surface confines monomers, intermediate oligomers and polymers in two dimensions and provides an anisotropic surrounding with spatially defined sites for reactivity (catalysis) and preorganization (templation). On the other hand, the atomically defined surface enables the detailed understanding of elementary chemical processes as it allows for analysis in real space by scanning probe microscopy. While in the (to the best of our knowledge) first polymerization experiment on a well-defined surface[16], spectroscopic techniques were used that average over large surface areas, local probing by STM became the method of choice. With the development of non-contact atomic force microscopy (ncAFM)[17], another method for molecule characterization has become available in recent years. By using highly defined functionalized tips, Gross and co-workers were able to resolve intramolecular bonds[18]. Thus, this method is capable of imaging

[1]Physical Chemistry Department, University of Graz, Graz, Austria. [2]Department of Chemistry, Humboldt-Universität zu Berlin, Berlin, Germany. [3]IRIS Adlershof, Humboldt-Universität zu Berlin, Berlin, Germany. [4]DWI – Leibniz Institute for Interactive Materials, Aachen, Germany. [5]Institute of Technicial and Macromolecular Chemistry, RWTH Aachen University, Aachen, Germany. *e-mail: leonhard.grill@uni-graz.at; hecht@dwi.rwth-aachen.de

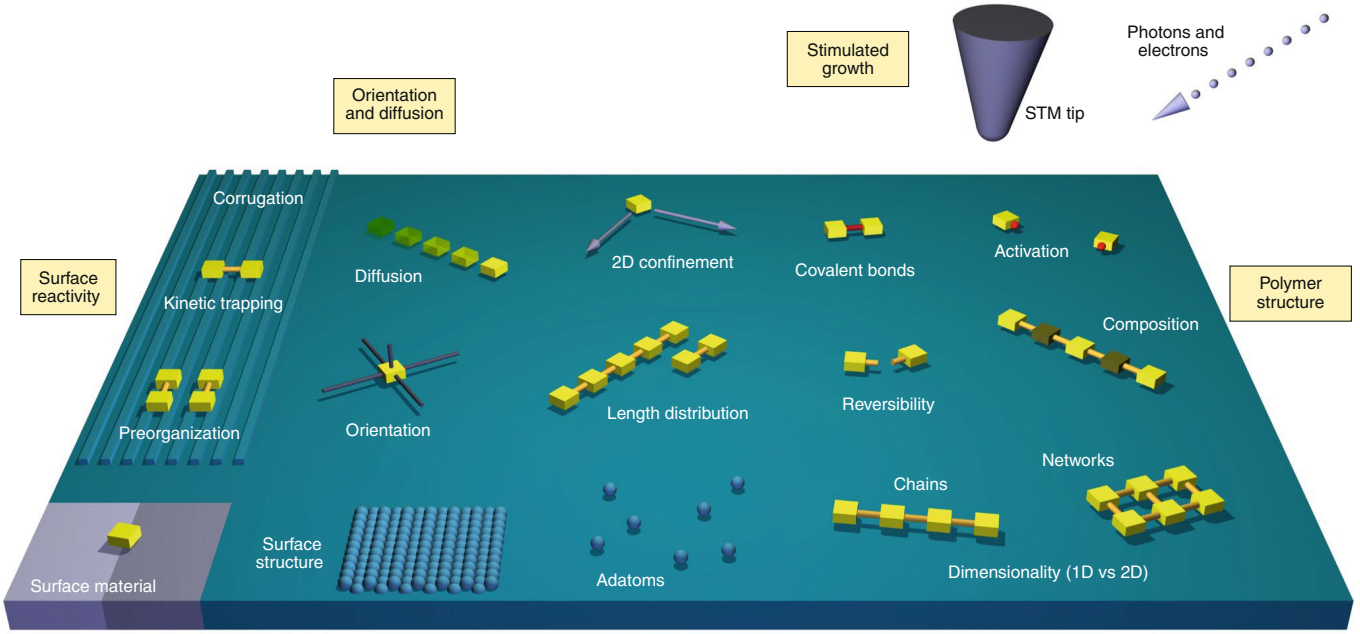

Fig. 1 | Key aspects of on-surface polymerization. Various topics that are discussed in this Review Article are shown schematically and are grouped according to the sections in which they appear.

the chemical structure of an adsorbed molecule in detail[19,20] and is well suited for on-surface polymerization by studying the precise structure of intermediate and final products, in particular for flat molecular systems.

The abilities of scanning probe microscopy to locally characterize the polymerization products in real space is accompanied by the drawback that polymers on a surface are typically not present in an amount sufficient to use conventional chemical analysis techniques, such as NMR spectroscopy and mass spectrometry. A rare attempt to combine the two approaches was reported by Stöhr, Mayor and co-workers, who compared covalent bond formation on a flat Cu(111) surface and on silver nanoparticles[13], using STM in the first case and mass spectrometry in the latter case. In addition, covalent on-surface coupling has been studied recently with quadrupole mass spectrometry and time-of-flight secondary ion mass spectrometry by starting from a saturated layer of precursor molecules on Au(111)[21]. Most studies on atomically defined solid substrate surfaces have been carried out under ultrahigh vacuum (UHV) conditions to provide very well-defined conditions and to exclude side reactions with the liquid or gaseous environment and contaminants therein, yet few polymerization reactions were induced on a solid/air[22] or solid/liquid[23,24] interface.

In the following sections, we will first emphasize crucial general considerations related to on-surface polymerization processes, before detailing key aspects related to the role of the surface as a 'reactive workbench' and the design of the monomer building blocks for generating a variety of polymer structures (Fig. 1). We critically discuss past and current achievements and finally provide an outlook with regard to both future scientific challenges and potential for application.

General considerations

Polymerization reactions taking place in the 2D confinement of a substrate surface are fundamentally different from the ones in the environment of bulk, solution or gas phase. The nature of the reaction mechanism used to link the monomers determines whether the polymerization proceeds in a step-wise fashion to form oligomers, which dimerize into larger oligomers and eventually assemble into polymers, as in typical step-growth polycondensation[25], or whether the polymerization occurs exclusively at the growing polymer chain end, leading to a linear growth of the molecular weight with increasing monomer conversion as in 'living' chain-growth polymerization[26]. Only the latter has enabled the control over chain length and dispersity as well as polymer architecture in solution[27]. Conventionally, the access of polymer structures has been limited for rather practical reasons, since the polymer product is typically characterized in solution and solubility has therefore to be maintained throughout the course of the polymerization. Hence, usually linear or branched polymers are being prepared while the introduction of even a small number of cross-links typically leads to insoluble amorphous polymer networks. These display the desired mechanical properties from elastic to plastic materials yet evade in-depth structural analysis due to lack of solubility and order.

In recent years, structurally well-defined 2D and 3D polymers with internal periodic order, which allows for structural insight by diffraction techniques, have become accessible by polymerizing monomers preorganized in a sheet-like fashion[14] and by dynamic covalent chemistry of rigid 3D building blocks[28], respectively. By confining the monomers to the solid substrate surface (as a monolayer), the resulting polymer structure is by default restricted to be planar, that is, ranging from linear polymer chains over intermediate ribbon structures to extended (open or closed) networks. Moreover, as the polymerization proceeds directly on the surface and analysis of the polymer products is typically performed in situ by STM or ncAFM, solubility no longer constitutes a restriction. For these reasons, on-surface polymerization has become an attractive and powerful method as it grants access to polymer structures that could not be prepared by other means.

When analysing the polymerization types (Fig. 2a) that have been explored on solid substrate surfaces, the majority of reactions have been polycondensation reactions involving the formation of small-molecule by-products in each coupling step. In solution, step-growth polycondensation yields polymers with typically rather low molecular weight and broad dispersity, yet if carried out in an iterative activation–coupling sequence with different monomers, it provides exquisite control over sequence[29]. On a surface, spatially

resolved activation by the STM tip as demonstrated by the seminal work of Rieder and co-workers[7] therefore in principle allows for unprecedented control over polymer architecture — a potential that has not been harnessed. In a few instances, polyaddition reactions have been realized in the context of dimerization of carbenes[30] or biradicals, either generated in initial cyclization reactions[31,32] or before deposition using a two-zone process[33], circumventing the generation of small-molecule by-products.

Formally, on-surface polymerization of such (globally) activated monomers proceeds via a step-growth mechanism, but in reality not much is known about the actual mechanism. In fact, as diffusion decreases substantially with increasing molecular size, growth is most likely occurring at the chain end or edge of the practically immobilized polymer chain or network by reaction with rapidly diffusing activated monomers (or short oligomers). Such a 'living' chain-growth scenario should be reflected in the typical linear evolution of degree of polymerization as a function of monomer conversion, but respective comprehensive experimental studies monitoring the chain length or network size as a function of coverage are lacking. In this context, we want to highlight the fact that with the exception of topochemical polymerization in diacetylene monolayers[34–36], chain growth, allowing for localization of reactivity at the chain end, has only been realized very recently by photoinitiating radical polymerization of preorganized maleimides on an insulator surface[37]. The scarcity of chain-growth on-surface polymerization arises because of the lack of suitable precursors — which are thermally stable during evaporation — and the limited linkage types that can be made on the substrate, which most importantly should not interfere with or quench chain propagation.

Thermodynamically, polymerization reactions typically suffer from a severe entropic penalty to the covalent linking of many monomer units, which lose their translational degrees of freedom, into one larger entity (note that there can be favourable entropic contributions from enhanced conformational degrees of freedom in ring-opening polymerization processes)[38]. To overcome this effect and achieve an overall reduction of Gibbs free energy of polymerization, enthalpy comes to the rescue as in a typical chain-growth polymerization, weaker C=C π-bonds are being converted into stronger C–C σ-bonds. These two opposing effects balance each other at a critical 'ceiling' temperature, below which enthalpy drives the polymerization and above which entropy drives depolymerization. In the confinement of the surface, however, the entropy of all reaction partners — including the monomers — is substantially reduced. Assuming adsorption energies to scale approximately linearly with increasing covered surface area and hence number of monomer units as well as similar enthalpic gain (due to the same covalent bond formation for all linking steps), step-growth polycondensation has the entropic advantage of producing small-molecule fragments as by-products (Fig. 2b) as pointed out in computational work by Oison, Humbel and co-workers[39]. As a remarkable consequence, this behaviour should give rise to a classical nucleation-growth mechanism[40], in which the initial formation of an oligomeric nucleus ('germ'[39]) is entropically disfavoured, but subsequent addition of monomer units to form larger polymeric structures occurs spontaneously with low barriers. Importantly, this suggests the possibility of realizing 'living' polymerization processes on surfaces — even when using conventional polycondensation chemistry.

Considering the kinetics during polymerization in the 2D confinement of solid surface, both the mobility and the reactivity of the (activated) monomers (and intermediate oligomers) are crucial steps that dictate the polymerization outcome. Depending on the properties of the surface and the monomer structure, as well as the linking reaction, the polymerization kinetics are limited by either diffusion or coupling at a given temperature (as sketched in Fig. 2c). This is nicely illustrated for the case of Ullmann coupling of aryl halides on coinage metal substrates[41,42]. On Cu(111), coupling reactivity is high, but the strong interaction with the monomers (and oligomers) leads to diffusion-limited polymerization. On Au(111), diffusion is much faster and the polymerization becomes limited by the coupling reaction. Disentangling these two features has, however, proven difficult and requires kinetic studies by analytical techniques with sufficient temporal resolution, such as fast X-ray photoelectron spectroscopy. These should be complemented by computational modelling and kinetic simulation as used in the collaborative efforts of the Perepichka, Rosei and Contini groups, who provided evidence for a nucleation-growth mechanism during an Ullmann-type polycondensation reaction[43]. Therefore, the polymerization can be controlled by tuning the nature of the substrate (composition and surface reconstruction) and the monomer (reactivity and adsorption properties) and by adjusting the substrate temperature.

In addition to sufficient diffusion, an increased surface coverage, that is, monomer density, enhances the polymerization. Note, however, that polymerization reactions have often been carried out with submonolayer coverage to facilitate analysis of discrete 1D or 2D objects by STM. Ultimately, the obtained degree of polymerization is governed by the extent of monomer conversion according to Carothers' famous equation and hence the size of the surface-bound polymer reflects the overall efficiency of the coupling reaction used (for more details, see 'Orientation and diffusion' below). Beyond diffusion and reactivity, one needs to steer the chemo- and regioselectivity of the monomer coupling steps during the on-surface polymerization process to fully control the resulting polymer structure with regard to dimensionality, topology and composition. The required selectivity can be achieved by the use of anisotropic, corrugated surfaces as well as specifically designed, sterically hindered monomers to favour specific reactions pathways.

The synthesis of new products on a surface requires a chemical modification of the monomer molecules, in contrast to supramolecular and organometallic molecular assemblies that are based on reversible interactions between unchanged species or metallic linker atoms, respectively. In most studies, dehalogenation of a suitable precursor has been used to create reactive sites within the molecules (namely the 'activation' step) that subsequently undergo covalent linking to other building blocks. It has been proposed that a surface-stabilized radical is formed[42] where the dehalogenated carbon atoms of the molecule form a chemical bond with the metal surface. The thus enhanced lifetime of the radical gives rise to efficient covalent linking. Note that isolated activated monomers — as sketched in Fig. 1 — are rarely found on the surfaces after thermal treatment[8]. The reactive sites in each molecule are precisely determined by the location of the halogen substituents in the initial precursor, which plays a crucial role as it is responsible for the atomic precision of on-surface synthesis. It allows for the creation of 1D chains, 2D networks or simple dimers from molecular building blocks, depending only on the number and position of halogen substituents in the initial molecular building blocks[8]. However, these positions are not always fixed as radical sites can migrate, for example, along the backbone of tetracene on Cu(110), reaching new positions within the molecule and thus different regiochemistry of monomer–monomer connection[44]. Recently, Xu and co-workers (using STM and ncAFM for imaging) employed more than one halogen substituent atom at the same location within the molecule, resulting in on-surface polymerization via double[45] and triple[46] carbon–carbon bonds if two or three Br substituent atoms are used, respectively. The following sections focus on the role of the solid substrate surface to steer the outcome of the polymerization process and subsequently discuss the types of polymer structures accessible by the on-surface polymerization technique.

Surface reactivity

The formation of covalent bonds in the vicinity of solid substrate surfaces is historically associated with the concept of heterogeneous catalysis[47] — widely used in the chemical industry — where

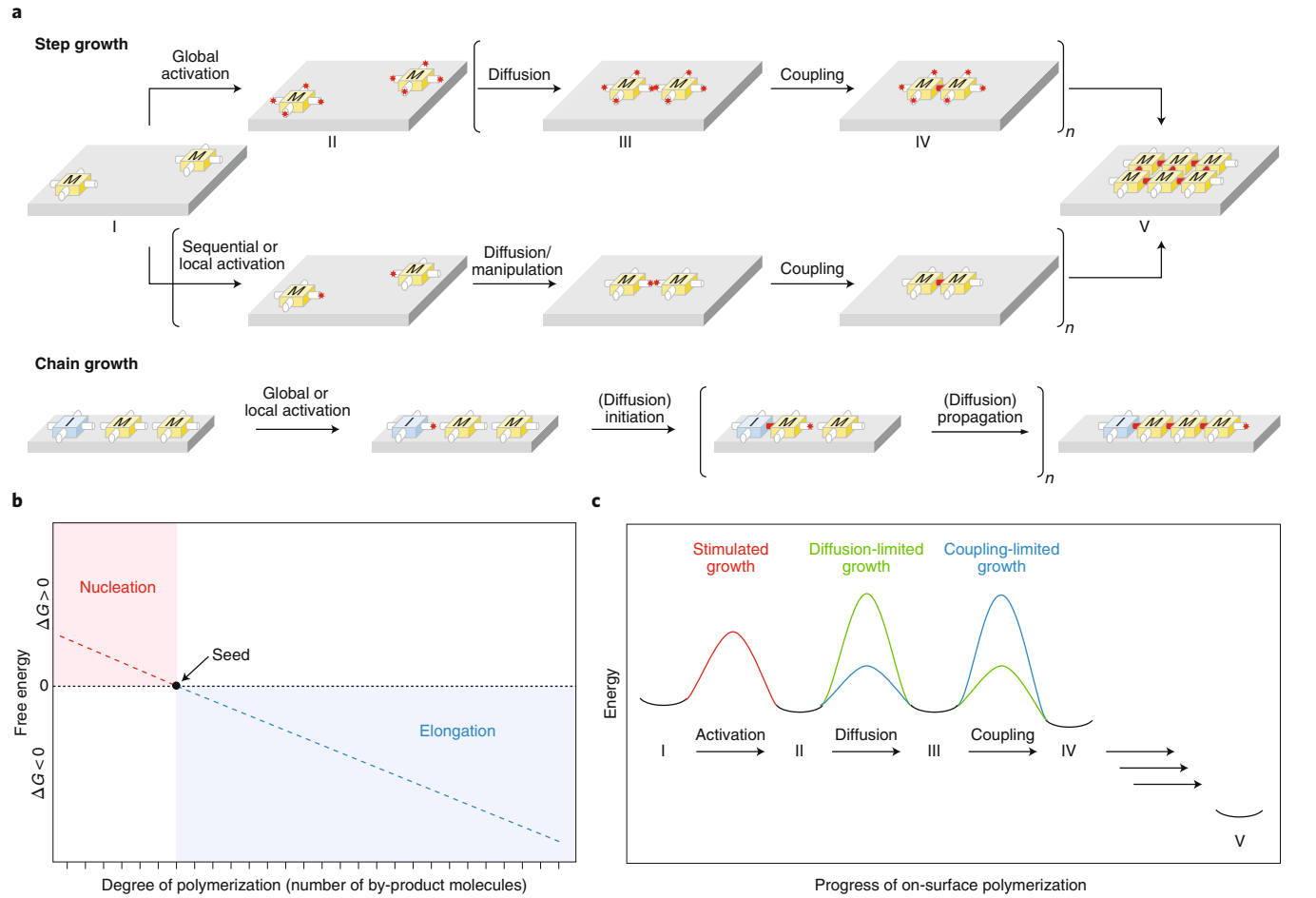

Fig. 2 | General mechanistic as well as thermodynamic and kinetic aspects of on-surface polymerization. a, Step-growth involving either global, sequential or local activation followed by diffusion/manipulation and coupling steps versus chain-growth involving global or local activation followed by initiation and propagation (in the case of preorganized monomers diffusion is not necessary). Sequential activation is based on chemoselective reactions, such as carbon–halogen bond dissociation, encoding orthogonal growth directions (see Fig. 5e). M, monomer; I, initiator. **b**, Entropic gain in the course of step growth due to release of small-molecule by-products can give rise to a nucleation-growth mechanism[39]. **c**, Growth processes can be induced by stimulated/catalysed activation and controlled by the relative rates of diffusion and coupling[41].

the products typically leave the surface after the reaction while they remain adsorbed in on-surface polymerization. The molecule–surface interactions dictate molecular mobility and hence reaction kinetics — yet, moreover, the surface often directly influences the mechanism due to its inherent catalytic activity, lowering activation barriers and associated temperatures. Various low-index noble metal surfaces, which are rather inert and therefore enable efficient diffusion, such as Au(111)[8,11,48], Au(100)[49], Cu(111)[30], Cu(110)[50,51], Ag(111)[52], Ag(100)[53] and Ag(110)[54] (Fig. 3a–c) have been used to link molecules by on-surface synthesis, in some cases comparing them directly[42,49,53–57].

A key parameter is the balance between adsorption energy and molecular diffusion. For instance, while dehydrogenative polymerization and cyclodehydrogenation occur for different polycyclic (hetero)aromatic hydrocarbons on the rather inert Au(111) surface (with efficient molecular diffusion), only the cyclodehydrogenation process was observed for the same molecules on the more reactive Pt(111) that strongly reduces diffusion[58]. Porte and co-workers have studied polymerization by dehydration of 1,4-benzenediboronic acid on copper, silver and gold surfaces and they found that Ag(111) (Fig. 3c) is the best compromise between mobility and adsorption strength[53]. On Cu(111), the molecules adsorb too strongly, leading to limited diffusion, while on Au(111) the molecule–surface interaction is too weak, resulting in early molecular desorption[53]. The same two surface orientations, yet different surface materials, lead to very different results for hexabenzocoronene coupling[55]. On Au(111), covalent coupling occurs at 420 K, whereas on the catalytically more active Cu(111), the molecules are spontaneously activated at room temperature, forming metal–ligand bonds with Cu adatoms (Fig. 3f) without any heating step. Subsequent heating of the Cu(111) surface at 450 K leads to molecular desorption and does not result in covalent polymers.

Besides the choice of the surface material, its orientation and therefore surface structure is crucial because this affects the catalytic activity of the surface. For instance, dimers and trimers of anthracene are formed by cycloaddition on Au(111), but only dimers are generated on Au(100) due to its surface corrugation[59]. While low-index surface orientations are preferred because they provide high mobility of the molecular precursors, the same surfaces typically exhibit lower catalytic activity, which is important for monomer activation and coupling. When using the stepped Au(10,7,7) surface for polymerization of dibromoterfluorene molecules, spontaneous Br dissociation at room temperature was found, which is absent on Au(111)[60]. The kink sites at step edges could be identified as catalytically active sites for the dehalogenation (the activation process is sketched in Fig. 3g).

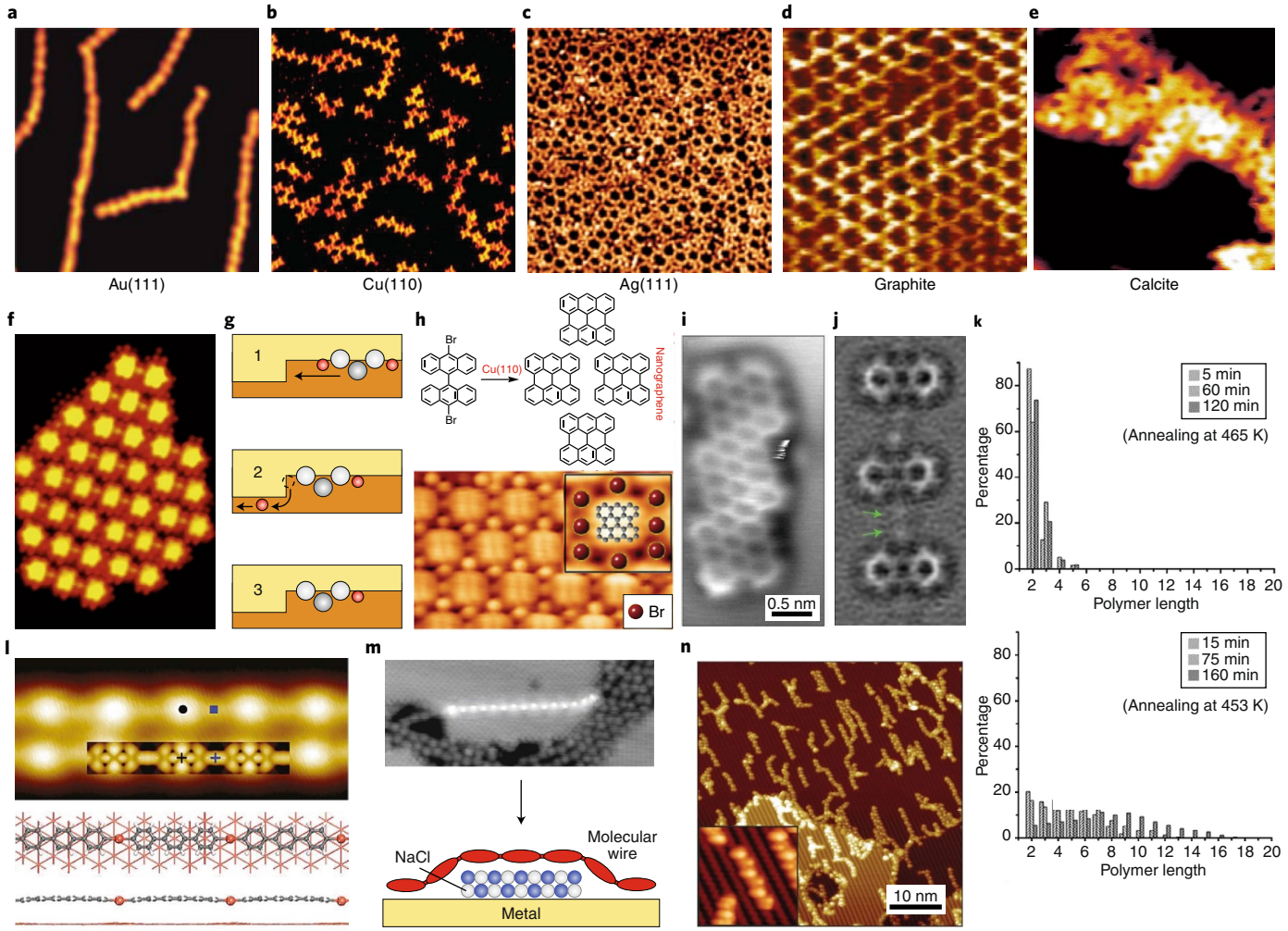

Fig. 3 | Role of molecule-surface interactions. a–**e**, After on-surface polymerization of porphyrin molecules on Au(111)[8] (image size: 30 × 30 nm^2) (**a**) and on Cu(110) (38 × 38 nm^2)[50] (**b**), polymerization of 1,4-benzenediboronic acid on Ag(111) (30 × 30 nm^2)[53] (**c**), boroxine networks on graphite (13 × 13 nm^2)[22] (**d**) and of benzoic acid polymers on an insulating calcite (11 × 11 nm^2)[74] (**e**). **f**, Hexabenzocoronene coupling via Cu adatoms (visible as small lobes between the bright molecules) on Cu(111) (10 × 15 nm^2)[55]. **g**, Schematic view of Br (in red) dissociation from molecular building blocks (white/grey) at kink sites on Au(10,7,7) (yellow)[60]. **h**,**i**, On-surface polymerization of bianthryl on Cu(110)[57] (8 × 5 nm^2) (**h**) and Cu(111)[65] (**i**). **j**, Anthracene oligomer with diacetylene units as linkers (indicated by green arrows) on Cu(111) (3.1 × 1.4 nm^2)[179]. **k**, Distribution of polymer lengths for Pd (top) and Cu (bottom) adatoms that act as catalysts to enhance reactivity for on-surface polymerization[73]. **l**, STM image (top) and calculated structure (bottom) with a calculated STM image (inset) of bis(aryl) Cu complexes as the intermediate product during polymerization (8 × 4 nm^2)[70]. **m**, Individual molecular polyfluorene wires on ultrathin insulating NaCl films (15.4 × 6.1 nm^2)[79]. **n**, On-surface polymerization of terfluorene on semiconducting TiO_2 (ref. [85]). Panels **a**–**d**, **f**, **h**, **l**–**n** are STM images; panels **e**, **i** and **j** are AFM images. Panels adapted with permission from: **a**, ref. [8], Springer Nature Ltd; **b**, ref. [50], RSC; **d**, ref. [72], American Chemical Society; **e**, ref. [74], American Chemical Society; **f**, ref. [55], Elsevier; **g**, ref. [60], Wiley; **h**, ref. [57], American Chemical Society; **i**, ref. [65], American Chemical Society; **j**, ref. [179], American Chemical Society; **k**, ref. [73], Wiley; **l**, ref. [70], American Chemical Society; **m**, ref. [70], Wiley; **n**, ref. [85], RSC. Panel **c** reproduced with permission from ref. [53], APS.

Another example is the growth of GNRs from one and the same 10,10′-dibromo-9,9′-bianthryl precursor on differently oriented copper surfaces. On Cu(110), no extended polymers but individual nanographene molecules were observed (Fig. 3h), due to the reactivity of the slightly corrugated Cu(110) surface that induces cyclodehydrogenation before Ullmann coupling[57]. This is in contrast to the flat Cu(111) surface where polymerization takes place and GNRs have been observed by different research groups who investigated the very same system of dibromo-9,9′-bianthryl on Cu(111)[57,61]. However, they interpreted their results differently, which resulted in a debate[62,63] whether the observed GNRs have a straight seven-armchair (similar to what has been observed on Au(111)[11] and Ag(111)[64]) or a chiral (3,1) structure. It was ncAFM with functionalized tips that solved this controversy. While in STM images[57,61] the characteristic kinks of chiral (3,1) GNRs are only weakly visible, ncAFM identifies them very clearly (Fig. 3i and Fig. 4l). This rather novel method was thus capable of clarifying the precise chemical structure of the products, which are not straight seven-armchair but indeed chiral (3,1) GNRs[65,66]. The strength of high-resolution ncAFM becomes furthermore evident in the on-surface polymerization of anthracene oligomers on Cu(111) where the diacetylene units that link neighbouring anthracene moieties can clearly be identified (marked by arrows in Fig. 3j).

In addition to its orientation, a metallic surface can also influence the polymerization process by providing adatoms. After activation of the molecules by thermal dehalogenation, they form metal–ligand bonds with single adatoms, either to a final product of the polymerization process[67] or as an intermediate species that is subsequently transformed into a covalently bound product by heating at higher temperatures[68]. This effect depends on the number of

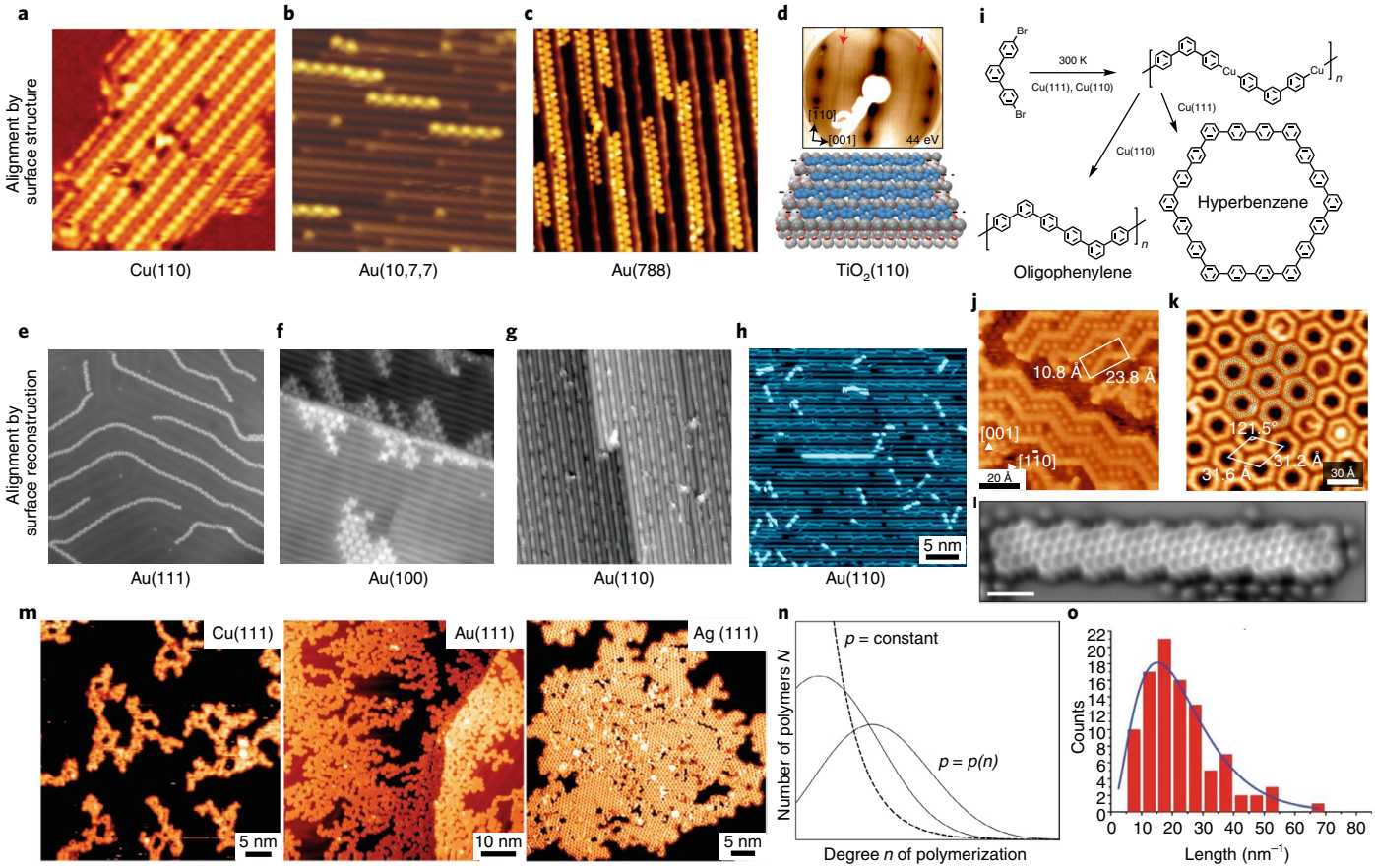

Fig. 4 | Molecular orientation and diffusion on the surface. a–c,e–h, Molecular nanostructures aligned either by the surface structure (PPP on Cu(110) (image size: 14 × 14 nm^2)[51] (**a**), polyfluorene on Au(10,7,7) (27 × 27 nm^2)[60] (**b**) and chevron-type GNRs on Au(788) (46 × 46 nm^2)[89] (**c**)) or by the surface reconstruction (polyfluorene on Au(111) (66 × 66 nm^2)[90] (**e**), porphyrin chains on Au(100) (42 × 42 nm^2)[49] (**f**), as well as polyethylene (28 × 28 nm^2)[91] (**g**) and polyphenyl[92] (**h**) chains on Au(110)). **d**, Ordered PPP chains as observed by low-energy electron diffraction on TiO_2(110) (sketch at the bottom)[93]. **i–k**, The formation of different phenylene oligomers depends on the surface orientation (as sketched in **i**)[94], with extended chains on Cu(110)[94] (**j**) and rings on Cu(111)[95] (**k**). **l**, Chiral GNRs grow on Cu(111), due to the precursor orientation. Scale bar, 1 nm (ref. [66]). **m**, Comparison of on-surface phenylene polymerization on different close-packed noble metal surfaces[42]. **n,o**, Polymer length distributions, simulated with an adapted Flory model (see text) (**n**) and measured for GNRs on Au(788)[89] (**o**), exhibit a characteristic maximum. Panels **a–h** and **j–m** are STM images; panel **l** is an AFM image. Panels adapted with permission from: **a**, ref. [51], Wiley; **b**, ref. [60], Wiley; **c**, ref. [89], APS; **d**, ref. [93], American Chemical Society; **e**, ref. [90], AAAS; **f**, ref. [49], Springer Nature Ltd; **g**, ref. [91], AAAS; **h**, ref. [92], American Chemical Society; **i,j**, ref. [94], RSC; **k**, ref. [95], Wiley; **l**, ref. [66], American Chemical Society; **m**, ref. [42], American Chemical Society; **o**, ref. [80], APS.

adatoms available to serve as linkers and thus the adatom diffusion barrier on the surface[69]. In some cases, reductive elimination from the intermediate bis(aryl) copper complexes (Fig. 3l) to the corresponding biaryl-linked covalent polymers could be observed[70,71]. Surface adatoms as side products can also be detrimental to the catalytic activity of the surface as observed at the solid/liquid interface where iodine atoms that are split off in the dehalogenation step can poison the Au(111) surface and therefore inhibit polymerization[72]. Although the metallic surface very often acts as a catalyst, this function can also be provided by adsorbed atoms, for example, Pd or Cu atoms on a Au(111) surface, leading to a lower activation energy in the presence of Cu compared with Pd (Fig. 3k), directly revealing the beneficial catalytic role of the adatoms[73].

Weakly interacting, typically insulating, surfaces represent a challenge for on-surface polymerization because molecules often bind too weakly. This results in low desorption temperatures, which are in contradiction to the much higher temperatures needed for molecular activation. Nevertheless, polymerization could be achieved on a catalytically inactive graphite surface (Fig. 3d)[22], because polymerization starts already at 120 °C where no desorption occurs. Higher polymerization temperatures are difficult to achieve on graphite surfaces — trimesic acid molecules, for example, desorb at 200 °C (ref. [22]). A direct comparison between noble metal and graphite surfaces thus revealed that, in accordance with the different adsorption energies, polymerization could be induced on the former whereas the molecular building blocks desorbed from the latter before any reaction took place[54]. On calcite, as another weakly interacting substrate, this desorption problem has been solved by Kühnle, Gourdon and co-workers by introducing carboxylic acid groups as 'anchors' to bind more strongly to the insulating surface (Fig. 3e)[74,75].

In contrast to bulk insulating samples, ultrathin NaCl films on a metallic substrate represent a particular setup[76], because molecular structures are decoupled from the metal underneath while scanning tunnelling microscopy and spectroscopy can be used. Such a metal–insulator–molecule setup can be achieved by transferring molecular nanostructures with the tip of an STM from metallic areas — where they were grown — onto thin NaCl islands[77,78]. However, the island height is limited since stable imaging becomes difficult on thicker NaCl films[79]. By depositing NaCl after the on-surface polymerization step, it turned out that the presence of molecular

nanostructures does not perturb crystalline NaCl growth. The NaCl islands simply repel the polymers on the surface until they (partially) adsorb on the NaCl islands (Fig. 3m). This particular configuration can be used for analysing charge transport through individual polymer chains[79]. In the case of on-surface polymerization on a boron nitride layer[80] on top of a Ni(111) surface, Pd and Cu atoms were deposited to catalytically induce the reaction, which occurs at lower temperatures than without the metal atoms[81].

Beyond insulators and metals, semiconductor surfaces include promising properties due to their relevance in technology. However, they have been used for on-surface synthesis only scarcely so far, because of their high reactivity that typically limits molecular diffusion and thus covalent linking. On Ge(001) for example, Br substituents dissociate already at room temperature whereas the same precursor molecules remain intact on hydrogen-passivated Ge(001)[82]. Heating of the latter at 450 K to induce molecular coupling causes hydrogen desorption from the surface and thus destroys the passivating hydrogen layer instead of polymerization[82]. If, however, aryl iodides are used on H-terminated Ge(001), polymerization becomes feasible. Accordingly, oligomers are formed — rather short though, due the limited temperatures (below 240 °C)[83]. If temperatures above 250 °C are used, the passivating hydrogen layer is destroyed again and consequently molecular diffusion and covalent linking is hindered. Hence, there is only a narrow window for on-surface synthesis. In addition, TiO_2 has been successfully used for linking of Br- and I-substituted bianthryl derivatives (Fig. 3n)[84,85], showing that the on-surface polymerization can indeed be applied to semiconducting surfaces. It turned out that the efficiency of the coupling reaction between the aryl halides is governed by the density of surface hydroxyl groups. In fact, polymerization does not occur in the absence of hydroxyl groups, pointing to a substantially different polymerization mechanism on TiO_2 compared with noble metals.

Orientation and diffusion

10,10′-Dibromo-9,9′-bianthryl precursor molecules have been used by Fasel and co-workers in their pioneering work to grow straight GNRs by on-surface polymerization via an Ullmann reaction and subsequent cyclodehydrogenation on Au(111)[11] (straight ribbons were obtained also on Ag(111)[64]). However, on another fcc(111) surface — Cu(111) — the Ullmann route is inactive for the same precursor, because the Cu(111) surface structure leads to a characteristic orientation of the precursor molecules with respect to each other before polymerization[61]. As a result, chiral — instead of straight — GNRs are formed as can be seen very clearly in ncAFM imaging[66] (Fig. 4l).

So far, free monomers that move in any direction on the surface have been considered. However, at the atomic level no crystal surface is isotropic and therefore molecular precursors always adopt specific adsorption sites and orientations that affect the polymerization reaction. Moreover, the conformation of each individual monomer building block on adsorption is important as it must enable a facile linking reaction. For instance, the efficient formation of *meso*-linked anthracene polymers can be achieved by the deposition of a suitable 10,10′-dibromo-9,9′-bianthryl precursor[11,86] with a twisted structure that is crucial for the polymerization since it reduces the steric hindrance between activated monomers. In contrast, simple anthracene monomers adsorbing in a flat geometry on the surface cannot link[87].

Anisotropic surface orientations, such as Cu(110)[50,51,88], and stepped surfaces, such as Au(10,7,7)[60] and Au(788)[89], can cause preorganization of the initial precursors and activated monomers as well as alignment of the intermediate and final polymerization products (Fig. 4a–c). However, different surface reconstructions can also be utilized to preorganize monomers and the resulting polymers (Fig. 4e–h shows (111), (100) and (110) facets of Au)[49,90–92]. A preferred orientation of long poly(*para*-phenylene) (PPP) chains has been achieved along the oxygen rows of the semiconducting TiO_2(110) surface (Fig. 4d) as shown by a combination of low-energy electron diffraction (averaging over large surface areas) and STM (local probing)[93]. The same PPP chains were shown to grow in a preferred orientation on the reconstructed Au(110) surface because the coupling reaction is confined in the surface troughs (Fig. 4h)[92].

By directly comparing the same 4,4′′-dibromo-*meta*-terphenyl precursors on two differently oriented copper surfaces, Cu(111) and Cu(100), Gottfried and co-workers observed oligo(*meta*-phenylene)s formation by Ullmann coupling on both (Fig. 4i–k).[94] On Cu(111), however, close-packed so-called hyperbenzene rings with a large diameter of 21.3 Å (Fig. 4k) were observed[95], whereas on Cu(110), non-covalent of assemblies of zigzag oligo(*meta*-phenylene) chains (Fig. 4j) were found[94]. Another strategy to pre-organize monomers relies in a non-covalent self-assembly before the polymerization reaction, using either metal–ligand bonds[96] or covalent linking in a preliminary step that results in a zipping process[49].

Molecular adsorption geometry can also affect diffusion[97], a key parameter for on-surface synthesis polymerization as it rules the supply of precursor molecules, activated monomers and intermediate oligomers. Thermal diffusion of these species can be completely suppressed as in the case of molecular monolayers[34,98] or chemisorbed molecules[88] that are linked with each other in a subsequent step.

Reactivity and diffusion both govern on-surface synthesis processes, each of them in very specific manner depending on the type of molecular building blocks, linking chemistry and surface structure. In fact, these two parameters typically compete, resulting in either coupling-limited or diffusion-limited processes (Fig. 2), depending on their relative energy barriers[41]. Diffusion-limited polymerization occurs for polyphenylene networks on noble metal surfaces. The different surface properties resulted in molecular networks of low density and branched, fractal-like structures on Cu(111), while much more regular and denser structures were found on Ag(111) due to the different kinetics of the involved diffusion and coupling steps as revealed by accompanying Monte Carlo simulations (Fig. 4m)[42]. However, coupling-limited polymerization was observed where either steric hindrance can inhibit efficient bond formation[87] or an improved orientation of the building blocks results in more efficient coupling[49]. Specifically, the number of defects decreases and the size of the networks increases if the reaction is carried out on Au(100) instead of Au(111), because the straight rows of Au(100) lead to a preferred parallel orientation of the intermediately formed oligo(porphyrin) chains (Fig. 4f)[49].

The statistical nature of the (covalent) coupling leads to chains of different lengths, that is, number of repeat units, when a polymer grows in a bottom-up fashion. To simulate a step-growth polymerization process according to Flory's model[99], we assume that monomers and intermediate oligomers exhibit equal reactivity at all stages. This means that the probability of an individual monomer to be reacted (between 0 and 1, depending on its reactivity and the experimental conditions) is equal to the total fraction p of all monomers that have linked. On the basis of these assumptions, the total number $N_n(t)$ of n-mers, that is, polymers that consist of n units, at time t is:

$$N_n(t) = n_o(1-p)^2 \times p^{n-1}$$

where n_o is the total number of monomers (available at the beginning of the reaction)[99]. It is composed of the probability p^{n-1} to find a chain of $(n-1)$ units and the probability $(1-p)$ that the final (nth) unit is unreacted (and therefore limits the chain length to exactly n). Thus, the length distribution of a *p*olymerization process results in an exponential decrease as plotted in Fig. 4n (dashed lines). Note that the distribution decays for all possible p values, showing that

the number of molecular chains consisting of only one unit is always the largest. This is because all oligomers grow in the same manner, that is, with equal reactivity (p = constant). Hence, while monomer coupling should raise the number of dimers, the number of trimers increases at the same time at the cost of dimers and so on.

On a surface, however, the situation changes, because the mobility of the growing polymer chains typically decreases with increasing size (as the diffusion barrier rises with the adsorption energy, which is approximately proportional to the polymer length). Hence, the probability p of an individual monomer to be reacted decreases with the oligomer length n. For simplicity, we assume a linear relationship: $p(n) = c_1 - c_2 \times n$ (with $c_{1,2}$ as constants) that results in a modified distribution (Fig. 4n). Specifically, a maximum appears that was absent before, that is, without surface. Hence, a certain polymer length should exhibit the highest abundance, in dependence of the function $p(n)$ that reflects the properties of molecules and surface and defines the position of the maximum (two examples are given in Fig. 4n). In experiments, the occurrence of such peaks in the polymer distribution has indeed been observed, namely for the on-surface polymerization of GNRs on a stepped Au(788) surface (Fig. 4o)[89] and on Au(111)[11], where the peak position was attributed to the dimensions of the Au(111) surface reconstruction. Furthermore, the maximum of the distribution could be shifted via the sample annealing temperature for nanostructures formed by metal-coordination bonds[100], illustrating the general validity of the Flory model modified by simple assumptions.

Polymer structure

The past decade has witnessed an explosion of the on-surface polymerization field as an increasing number of chemical reactions have been utilized to successfully link molecular building blocks on various, particularly metal, surfaces. A recent comprehensive overview of all chemical transformations explored in on-surface synthesis is given by Fuchs and Studer[101]. Here, we want to focus on important structural aspects in the context of polymers, in particular focusing on control over the nature of the backbone, its dimensionality and composition.

Initially, a lot of research was — and still is — being devoted to the formation of stable C–C connections and in particular aryl–aryl connections due to the attractive electronic properties of the resulting conjugated polymers. While the first coupling of an aryl halide precursor, that is, iodobenzene, on Cu(111) has been investigated by Xi and Bent using (averaging) spectroscopic techniques back in the early 1990s[16,102], it was the group of Rieder that provided the first spatially resolved insight into this STM tip-induced, surface-assisted Ullmann reaction in their landmark paper[7] (see Fig. 7 below). These observations enabled the development of the dehalogenative aryl halide coupling into a successful polymerization technique[103]. The group of Weiss was the first to investigate a real monomer, that is, 1,4-diiodobenzene, on Cu(111) and described the formed chains as 'protopolymers'[104] (Fig. 5a), yet only later the team of Rosei and Perepichka studying the same monomer on Cu(110) could unambiguously demonstrate the formation of PPP[51]. This method has since then been used to prepare a variety of π-conjugated polymers, such as polythiophenes[51,88] or polyfluorenes (Fig. 5a)[90], which in some cases serve as precursors for extended ribbon structures (see below). In addition to C–X (X = halogen), also C–H bonds can be activated as demonstrated by the coupling of activated alkynes[105] or benzylic positions[50]. In the specific channel-type confinement of a Au(110) surface, it is even possible to selectively dimerize unactivated alkanes at their termini[91], a reaction that cannot (yet) be accomplished in solution. In contrast, radical polymerization — a reaction extremely common in solution and in bulk — has only very recently been accomplished on an inert KCl surface (Fig. 5b)[37], illustrating the dramatic differences between polymerization processes under conventional versus on-surface conditions.

Beyond carbon–carbon bonds, heteroatom-containing connections have been used to polymerize monomers on surfaces, for example, in the formation of polyesters[106], polyimides[107], polyimines[108], polyimine ribbons[109], as well as polyboroxines and polyboronates[52,110], among others. While all the above polymers are formed by polycondensation-generating by-products, such as halides, dihydrogen and water, few polyaddition reactions have been developed and are based on the dimerization of either carbenes[30] or diradicals formed by cyclization of enediyne precursors[31,32] and thus these reactions proceed also by a step-growth mechanism.

Over the past decade, many types of polymers, in which monomer units are connected via single covalent bonds, providing some degree of flexibility to the resulting 1D chains, have been reported. However, the growth of ordered 2D network structures requires additional strategies to overcome the associated entropic penalty (discussed above). One approach has been the folding of single chains using non-covalent interactions, such as hydrogen bonds, between the chains, as pioneered by van Esch and de Feyter on highly oriented pyrolytic graphite[111] and used in the case of polyamides on Ag(111)[112]. While this strategy gives rise to a surface-supported secondary structure, the covalent capture of appropriately folded polymer chains on a surface has proven to be an extremely successful strategy for the formation of ribbons, formally defined as ladder-type polymers, which constitute intermediates on the way from 1D to 2D structures. Their synthesis involves sequential connection, first in an intermolecular fashion (polymerization) and subsequently intramolecularly by cyclization within the same chain. Arguably, the most impressive examples for this approach have been described by the team of Fasel and Müllen in their landmark synthesis of zigzag (Fig. 5c)[12] as well as armchair (Fig. 5d)[11] GNRs. Due to their flat, truly 2D chemical structure, GNRs are highly suitable to being studied with ncAFM at high resolution. This technique allows imaging of the chemical structure, thus giving direct insight into the atomic composition of various types of GNRs[12,65,66,113,114] (as shown in Figs. 3i, 4o and 5c). Using appropriately designed monomer building blocks, the resulting ribbons' edge structure, width as well as composition can be controlled. A potpourri of nanoribbons has been made ranging from polyrylenes as the thinnest possible ones[115] to wide and (hetero)aryl extended ribbons[116,117] as well as N-doped[118,119] or B-substituted[120,121] GNRs. All these GNR structures, however, have a finite extension in the second dimension.

True 2D polymer networks have been prepared by polymerizing multifunctional monomers of four-fold or six-fold symmetry, such as tetra-brominated (metallo)porphyrins[8,122], 1,2,4,5-tetracyanobenzene to form a phthalocyanine network on the surface[123] or hexaiodinated cyclohexa(*meta*-phenylene) macrocycles to form 'porous graphene'[42,124]. The networks formed by these direct approaches, however, suffer from their limited extension in both dimensions, which can primarily be attributed to the difficult steric accessibility of reactive sites, reflected in narrow trajectories for the incoming activated monomer and thus low probabilities for productive collisions with the growing network. Note that successful network formation includes both branching but also closing of the loop and it is the latter that appears both kinetically as well as thermodynamically challenging[42,49,125]. A way to overcome this obstacle is to make use of sequential reactions in combination with the templating effect of the intermediately formed 1D structures. In one approach, preformed GNRs[11] can be fused at their armchair edges by thermal annealing either on Ag(111) (Fig. 5c)[64] or on Au(111)[126] and there have been early indications on the feasibility of dehydrogenation between oligophenyls[127]. In another approach, the chemoselectivity in C–C coupling reactions between aryl bromides and iodides has been exploited to first polymerize in one dimension (by preferably activating the more reactive linearly oriented C–I bonds in the 5,15-bis(4-iodophenyl)-10,20-bis(4-bromophenyl)-porphyrin monomers) and subsequently activating the orthogonally positioned

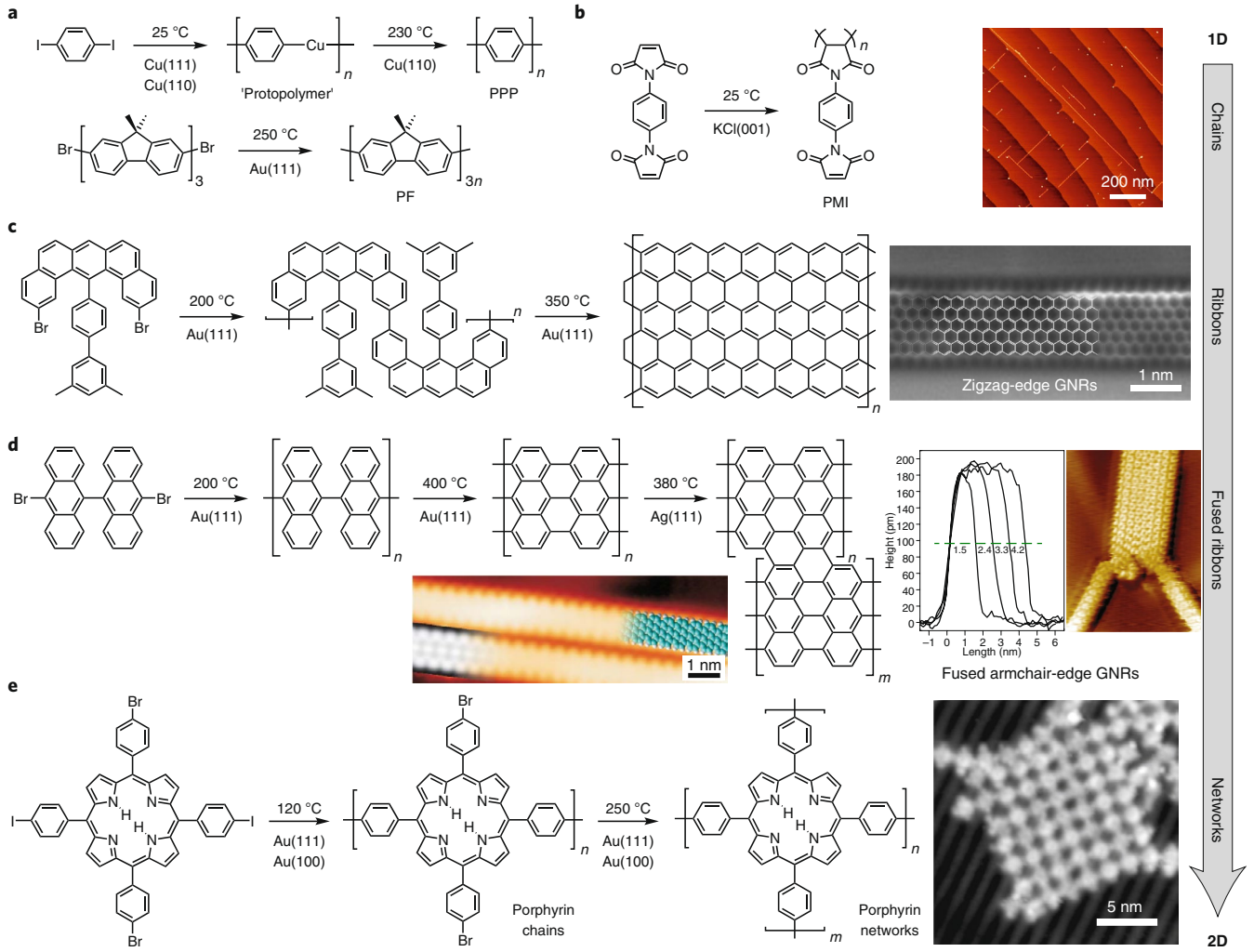

Fig. 5 | From 1D to 2D structures. a,**b**, Step-growth polymerization of dihalide precursors provides π-conjugated polymers such as PPP[51,104] and polyfluorene (PF)[90] (**a**) and chain-growth polymerization of a maleimide monomer gives saturated polymaleimide (PMI) chains[37] (**b**). **c**,**d**, Chain polymerization followed by intramolecular cyclization steps yields either zigzag[12] (**c**) or armchair[11] (**d**) GNRs, which can be fused to wider ribbons by thermal annealing on a different surface[64]. **e**, Sequential activation of a dibromo-diiodo-porphyrin precursor allows for initial linear polymerization followed by orthogonal cross-linking of the preorganized chains to provide polyporphyrin networks[49]. Panel **b** is an AFM image; panels **c**–**e** are STM images. Panels adapted with permission from: **b**, ref. [37], Springer Nature Ltd; **c**, ref. [12], Springer Nature Ltd; **d**, centre, ref. [11], Springer Nature Ltd; right, ref. [64] under a Creative Commons licence (http://creativecommons.org/licenses/by-nc-nd/3.0/); **e**, ref. [49], Springer Nature Ltd.

bromide side groups in the preorganized 1D chains to cause 2D network formation (Fig. 5d)[49]. The importance of preorganization has nicely been demonstrated by Lin and co-workers by supramolecular templating using coordination bonds between pyridine-terminated porphyrins[96]. While the C–I/C–Br chemoselectivity on Au(111) has also been used to assemble hexagonal networks[125], on an insulating calcite surface the reactivity difference between aryl bromide and chloride has been exploited to link monomers sequentially[75]. Using the above strategy of hierarchical bottom-up assembly, nanoporous graphene has very recently been synthesized via a new three-step sequence of C–Br Ullmann-type coupling followed by cyclodehydrogenation and final C–H coupling[128].

Despite these sophisticated growth approaches, the extension of the formed 2D networks remains rather limited, primarily due to irreversibly incorporated defects that prevent further growth. Thus, it is imperative to involve polymerization reactions under thermodynamic control to allow for defect healing. Initial work by Linderoth and co-workers involved imine formation, however, in UHV under non-equilibrating conditions[48], and hence kinetically trapped cycles among other species were formed[108]. The same holds true for boroxine formation[52], and probably the majority of chemical reactions under typical UHV conditions. It was Lackinger who first showed the importance of equilibration to heal defects[22,129] and could exploit boroxine formation under thermodynamic control also for larger aromatic bisboronic acid monomers to grow extended covalent organic framework layers on the surface[130,131].

Most polymers that have been prepared via on-surface polymerization are composed of one and the same repeat unit. The main reason for this prevalence is that the majority of the transformations employed during step growth are typically homocouplings, that is, involving a reaction between two identical chemical functionalities. Thus, it is difficult to run a classical $A_x + B_y$-type polycondensation between two distinct monomers, which then strictly alternate in the formed polymer chain/network. There are only a few examples involving two monomers containing different coupling functionalities[106,107,109,132], perhaps the most prominent case presented by 1,4-benzenediboronic acid as the linear A_2 monomer connected via 2,3,6,7,10,11-hexahydroxytriphenylene as the trigonal B_3 branching units (Fig. 6e)[52]. This particular monomer combination has historically been particularly successful as Côté and Yaghi used it to

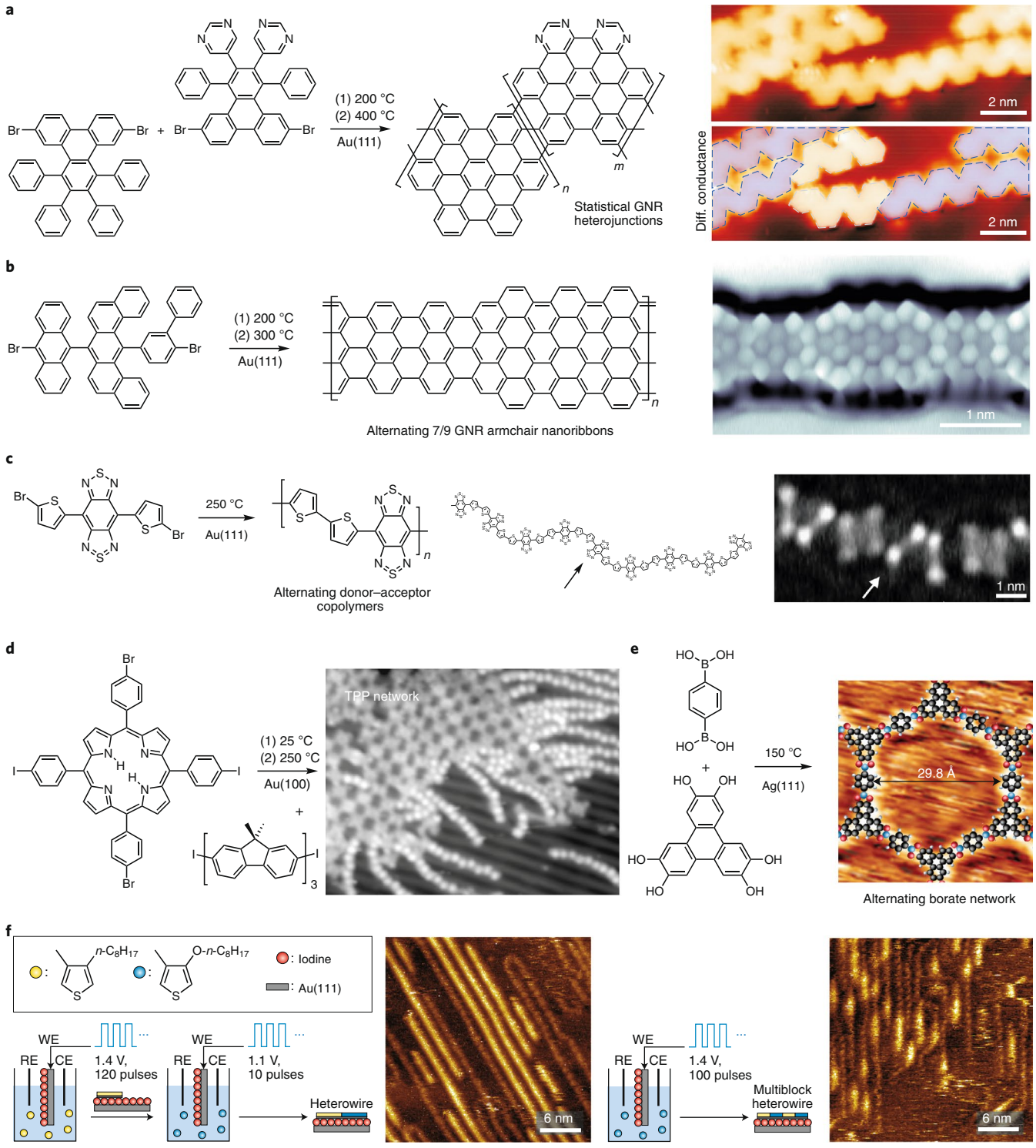

Fig. 6 | Random, alternating and block copolymer structures. a, Random copolymerization of two different dibromo-precursors followed by annealing provides N-doped chevron-type GNRs[119]. **b**,**c**, Homopolymerization of non-symmetrical dibromo precursors proceeds with high regioselectivity to give armchair GNRs of alternating width[135] (**b**), while homopolymerization of symmetrical dibromo precursors yields alternating donor–acceptor π-conjugated polymers as flexible low-gap molecular wires[136] (**c**). **d**, Sequential copolymerization gives rise to blocky 2D structures composed of porphyrin networks with polyfluorene chains[49]. **e**, Polycondensation of linear bisboronic acid and trigonal branching diol unit generated strictly alternating hexagonal network[52]. **f**, Copolymerization of more or less electron-rich thiophene monomers at different oxidation potentials gives rise to epitaxial growth of diblock (left) as well as multiblock (right) copolymers (WE, working electrode; RE, reference electrode; CE, counter electrode)[23,137]. Panels **a**–**f** show STM images. Panels adapted with permission from: **a**, ref. [119], Springer Nature Ltd; **b**, ref. [135], Springer Nature Ltd; **c**, ref. [136] under a Creative Commons licence (http://creativecommons.org/licenses/by/4.0/); **d**, ref. [49], Springer Nature Ltd; **e**, ref. [52], American Chemical Society; **f**, ref. [137], AAAS.

prepare the first porous crystalline covalent organic frameworks[133], sheets of which Dichtel and co-workers later grew on graphene[24].

Limited to conventional symmetrical coupling approaches, control over the incorporation of different monomers could only arise from reactivity differences, that is, reactivity ratios as in conventional copolymerization, and different dosing and diffusion. In principle, proper steric constraints should be able to prevent the homocoupling of one monomer, effectively forcing it to connect to the other monomer, which however is able to homopolymerize and form blocks. Thereby, a junction is being formed between blocks and one could refer to it as a copolymer that is enriched in one monomer, that is, blocky. This strategy has been used to create chevron-type GNR junctions resembling three-arm star polymers[11].

Steric inhibition of the homocoupling step is actually a common pitfall that controls and often prevents on-surface polymerization, as has been shown for GNRs where a twisted biaryl structure is essential for efficient coupling[55,113]. In case of frustrated homocoupling, the reactive centre can also migrate as reported for the polymerization of the 10,10′-dichloro-9,9′-bianthryl monomer, which due to the high thermal barrier for chlorine activation first undergoes cyclodehydrogenation thereby preventing direct coupling and leading to a radical shift[113], and also documented for the dimerization of dibromotetracene[44]. Linear junctions have been prepared between N-doped and all-carbon monomers, leading to multiple p–n junctions within chevron-type GNRs (Fig. 6a)[119]. However, no particular preferences for block-type structures were found and the prepared nanoribbons resemble statistical copolymers. The same is true for the recently published copolymerization to access edge-extended armchair GNRs[134]. A conceptually different approach relies on the use of properly designed monomers, which on homopolymerization form chains or ribbon structures, which resemble strictly alternating copolymers. For example, in related work on topological phases, armchair GNRs of alternating width have recently been accessed by regioselective head-to-head and tail-to-tail coupling of non-symmetrical α,ω-dibromoteraryls (Fig. 6b)[135]. To circumvent potential formation of regioisomers, our own groups had previously utilized symmetrical donor–acceptor–donor dibromo monomers for the synthesis of alternating donor–acceptor π-conjugated polymers as flexible molecular wires (Fig. 6c)[136].

Utilizing the different activation energies for halide dissociation, a sequential growth method (Fig. 5d) was realized to also prepare block-type heterostructures from porphyrin and fluorene monomers[49]. Initial selective homopolymerization of the porphyrins into linear 1D structures is followed by preferred attachment of the formed polyfluorene segments in the side chain, first forming comb-type structures, which after annealing on the corrugated Au(100) surface give rise to 'hairy networks' as a new and unprecedented type of block copolymer (Fig. 6d). True linear block copolymers have thus far successfully only been prepared by epitaxial growth on the surface of an Au(111) electrode in the pioneering work of Sakaguchi and co-workers[23,137]. Exploiting the different oxidation potentials of alkyl- and alkoxy-substituted thiophene monomers, they were able to prepare diblock copolymers, that is, 'heterowires' (Fig. 6f, left), and even (random) heteroblock copolymers, that is, 'multiblock heterowires' (Fig. 6f, right), using electrochemical deposition followed by STM visualization[137].

Stimulated growth

In the previous sections, we have illustrated how the obtained polymer structures can be controlled both by the nature of the surface as well as the monomer building blocks. In addition, externally addressing the specific site, where (and possibly also when) the polymer is being formed, will enable the realization of localized complex growth processes. This would merge the hitherto described chemical bottom-up approaches with state-of-the-art physical top-down approaches and thus promises an exquisite, if not the ultimate, control over the resulting covalent nanostructures. For this purpose, a suitable stimulus with high spatial (and proper temporal) resolution is needed and there have been promising reports, mostly using the tip of the STM itself[7,34–36,138] as well as electron[138] or light[139] sources. The latter has been realized with ultraviolet light, which was used to generate PPP on Ag(111) at room temperature[140].

Chemical reactivity induced in the tunnelling junction of an STM[141] was first used by Rieder and co-workers to induce the dimerization of iodobenzene (Fig. 7a)[7] and was envisioned by him as a way to practice 'molecular surgery' in the future[142]. However, while also the oxidation of single CO molecules could be realized[143], the rational step-by-step construction by moving, activating and connecting individual monomers on a surface has only scarcely been explored since then, due to the time-consuming nature of these serial processes involved in each individual connection step. Tip-induced polycondensation has been described involving the transformation of hydrogen-bonded lamellar islands of 1,4-benzenediboronic acid into the corresponding covalent boroxine networks[138]. In this case, the STM tip was used to locally create a polymerization nucleus, which subsequently propagates converting the hydrogen-bonded precursor phase into the covalently bonded polymer phase. The kinetics of this transformation are sufficiently slow to allow for monitoring by STM; however, they can be substantially accelerated by exposure to an e-beam (15 eV for 20 s), presumably due to formation of more reactive charged species caused by excitation of the underlying Ag(111) substrate. Recently, voltage pulses from an STM tip have been used to induce the collision of individual CF_2 fragments on a Cu(110) surface and it was found that their addition occurs only if the target molecule is on the trajectory of the incoming fragment, resulting in formation of C_2F_4 and thus en route to Teflon[144].

In contrast to step growth, chain-growth polymerization of appropriately organized monomers would require control over only the initiation step while subsequent polymerization proceeds without the need for further stimulation. This concept was first demonstrated by Okawa and co-workers for self-assembled monolayers of 10,12-nonacosadiynoic acid on graphite surfaces (Fig. 7b)[34,35]. Proper preorganization of the monomers enabled topochemical polymerization of the diacetylene units[145] after local initiation with the STM tip to give poly(diacetylene) wires, which were terminated by defects in the monolayer. One decade later, a team led by the same author took this concept one step further and reported on heterostructures that they created using the same diacetylene-containing monolayers but in the presence of phthalocyanine molecules[36]. After tip-induced initiation and propagation along the aligned diacetylene monomer rows, the reactive carbene chain end was not terminated at the 'defect', which happened to be the phthalocyanine molecule, but covalently connected presumably via C–H insertion (Fig. 7b). This so-called 'chemical soldering' provides perhaps the most impressive example thus far to create distinct and non-periodic molecular nanostructures combining top-down and bottom-up methods. Diacetylene polymerization has also successfully been carried in monolayers of slightly shorter 10,12-pentacosadiynoic acid monomers on an epitaxial graphene surface using photons[139]. Light as a mild yet global initiation method has also recently been used to trigger the radical polymerization of maleimide-containing monomers pre-organized on an insulating KCl surface (Fig. 5b)[37].

Scientific challenges and future prospects

Future developments of the field will heavily depend on an in-depth understanding of the elementary physical and chemical processes occurring during on-surface polymerization. This should include microscopic as well as spectroscopic tools to characterize reaction products and possibly intermediates, ideally with atomic resolution. The latter will become essential when new on-surface reactions, lacking a solution-phase analogue, give rise to new products with

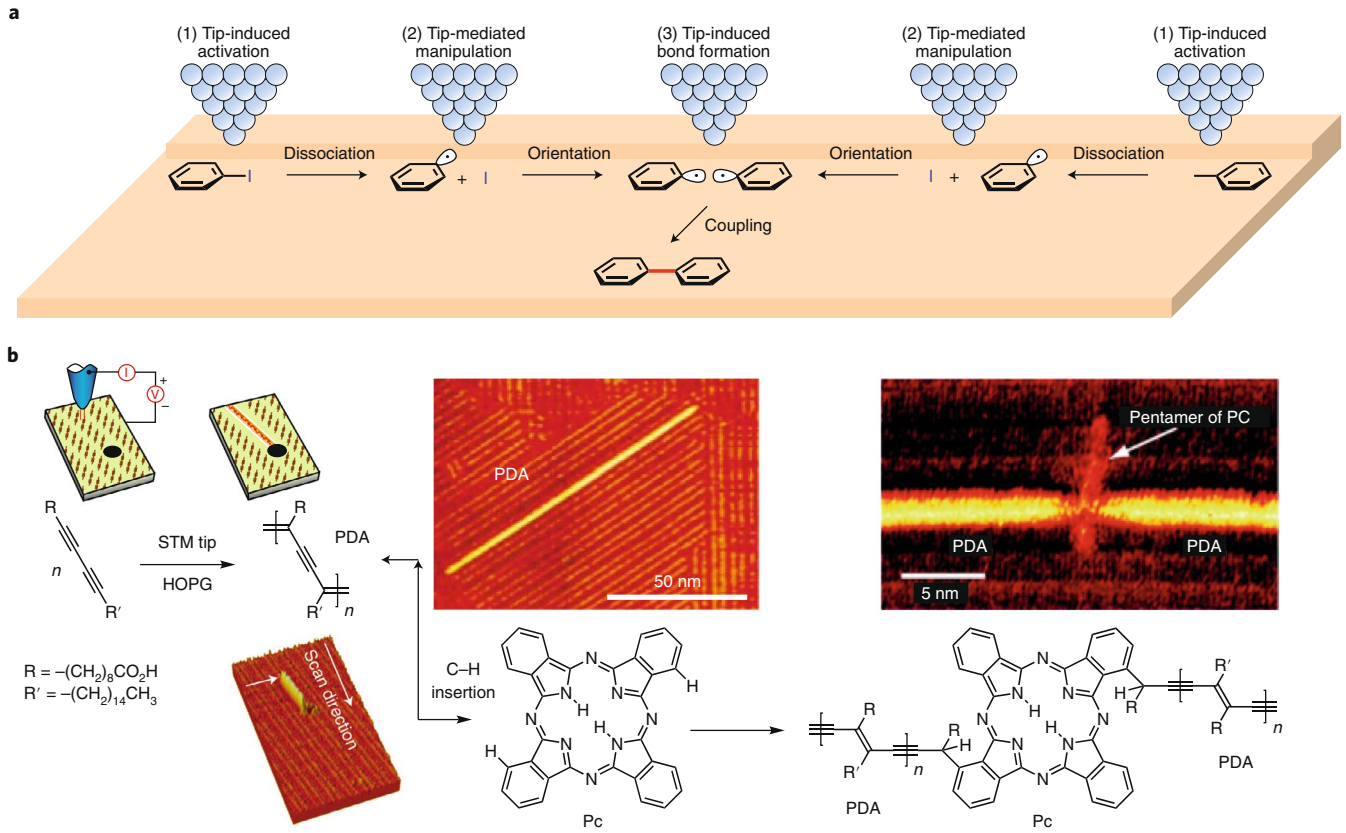

Fig. 7 | Controlling local covalent bond formation and chain-growth polymerization. a,**b**, Using the STM tip to induce the coupling of two iodobenzene moieties to generate biphenyl en route to polyarylenes[7] (**a**) and the chain-growth polymerization of pre-organized diacetylenes to generate poly(diacetylene) (PDA), which can be terminated at predefined defect sites[34,35] or intentionally placed phthalocyanine (Pc) moieties on highly oriented pyrolytic graphite (HOPG)[36] (**b**). Panel **b** adapted with permission from: left, ref. [34], Springer Nature Ltd; centre, ref. [35], AIP; right, ref. [36], American Chemical Society.

unexpected connectivities[146]. Developing these techniques even further to monitor structural changes in situ as the polymerization is proceeding will enable valuable insights into the reaction dynamics to be obtained[147]. Additional information can be gained by pulling the molecular constructs off the surface to map electrical, mechanical, electronic as well as optical properties using STM[86,90,148,149] and AFM[150–152], respectively. Equally important are new techniques that allow for the investigation of new substrate surfaces. Thus far, the field has been largely limited to readily accessible coinage metal substrates that can easily be analysed by STM due to their conducting nature. Alternative approaches have been emerging, such as ncAFM, which provides atomic resolution even on non-conducting surfaces[153]. However, the types of surfaces are still rather limited in combination with on-surface polymerization since the thermal treatment, required for covalent bond formation, can cause difficulties (see 'Surface reactivity'). We believe that photoinduced, hence remotely controlled, on-surface polymerization is a very promising approach, avoiding thermal treatment and at the same time providing exquisite selectivity via the choice of the photon source. Complementing the use of new substrate surfaces should also be an exploration of new reaction conditions beyond UHV. In this context, the two-zone chemical vapour deposition procedure developed by Sakaguchi and co-workers is promising as it separates the activation from the polymerization steps[33].

Beyond instrumentation and method development, a deeper understanding of the electronic properties of the generated π-conjugated polymers hybridized with the underlying metallic or semiconducting substrate is required to correctly interpret the obtained spectroscopic signatures. For example, the electronic structure of PPP has been studied on Cu(111)[154] and on Cu(110), exhibiting a quasi-1D metallic character on the latter[155], whereas on TiO_2(110) the band structure of PPP shows highly dispersive bands characteristic of a substantial overlap between the repeat units along the π-conjugated polymer[93]. Moreover, the on-surface polymerization of 1,3,5-tris(4-carboxyphenyl)-benzene via decarboxylation has been studied on Cu(111) by following the electronic structure from the monomer to the 2D covalent network[156]. The latter example illustrates that in contrast to linear π-conjugated polymers, which are reasonably well understood, there is still a lack of electronic structure theory for 2D π-conjugated polymers, which would substantially aid their design for optoelectronic applications[157–159].

In addition to the established synthetic pathways, new conceptual approaches are needed and are most likely to be found in the synergy of molecular and surface chemistry. Clearly, improved catalytic systems, for example, consisting of single Pd atoms on exfoliated graphitic carbon nitride[160] will continue to emerge and should become valuable for on-surface polymerization. In addition to the catalytic role of the substrate, the inherent order of a specific surface could be utilized to direct molecular polymerization processes by steering chemical reactivity and selectivity. Along this line, the seminal work by Wolkow on the self-directed growth of styrene lines on H-terminated Si(100)[161] serves as an impressive inspiration, although formally no connection occurs between the monomer units and hence no polystyrene is being formed. Another noteworthy collective effect in chain-like assembly structures has been reported by Yates, who observed a propagating reaction along dimethyldisulfide chains on Au(111) and Au(110)[162].

Complementary to these approaches based on an intrinsic reactivity modulation at the molecule/substrate interface, external stimuli provide remote control over local reactivity, as illustrated by photo- or tip-induced chain-growth polymerization[34–37,139] highlighted above. Such top-down controlled bottom-up nanofabrication has the promise to connect different monomers into sequence-specific, non-periodic 2D structures, hardly (if at all) accessible via conventional synthesis. Moreover, it is fair to state that structural complexity with regard to backbone heterogeneity, that is, copolymer type, has thus far also been limited. In this context, complementary metal–ligand interactions can be used to enhance the structural and compositional complexity as demonstrated by Amabilino, Raval and co-workers[163].

Extending into the third dimension is another promising direction to take, as illustrated by the advent of surface-mounted metal–organic frameworks developed by Wöll and co-workers[164]. In their work, they exploited epitaxial layer-by-layer growth of metal–organic frameworks on top of surfaces covered by self-assembled monolayers. Similarly, 2D networks grown by on-surface polymerization as discussed above could serve as templates from which to construct new 3D frameworks, for example, using metal coordination or possibly even by (dynamic) covalent bonds.

The technological relevance of on-surface polymerization thus far arises mainly from the production of large graphene sheets on metal surfaces by decomposition of carbon-containing molecules (as ethylene, propene, benzene, among others) and the polymerization of the fragments on the surface[165]. In a similar fashion, single 2D layers of boron nitride are formed on a metal surface by decomposition of borazine molecules[166]. These examples illustrate that on-surface polymerization is conceptually related to chemical vapour deposition, although during the process the organic precursor structure is typically not incorporated into a polymeric product but lost. In both cases, the product is generated where it is needed and thus removal of the underlying substrate to prepare non-supported 1D or 2D structures is typically not intended, and moreover problematic due to their insoluble nature. There have, however, been some attempts to transfer them from the substrate where they were grown to another[11]. In addition, there have been efforts to move on-surface polymerization closer to producing GNRs not in ultrahigh but 'ordinary' vacuum[167] and even at ambient pressure[168]. The latter example is important as it illustrates a common drawback of many studies since the nanostructures prepared by on-surface polymerization typically never leave the UHV chamber. Thus, the preparation of robust constructs, which are subsequently investigated with regard to their function under ambient conditions, should be pursued more frequently, despite the associated experimental difficulties.

There is certainly potential for porous 2D materials grown via on-surface polymerization approaches as they provide superior control over the dimensions, spacing and nature of the pores. However, two considerable obstacles have to be overcome before realizing such ideal membranes. On the one hand, the 2D networks have to be grown much larger and defect free and this will only be possible by using reversible coupling reactions under thermodynamic control as highlighted herein for some 2D networks based on boronic esters[22,129,130]. On the other hand, the underlying support has to be removed and free-standing sheets isolated as discussed above. Beyond using the inner voids as pores, 2D polymers and materials thereof can also serve to organize catalytically active sites relative to each other in space. For realizing and studying complex catalytic processes, which involve multiple steps at distinct and chemically incompatible sites, such well-defined architectures are highly attractive[169]. In related studies using 2D metal–organic frameworks[170] promising nonlinear effects have been revealed for the oxygen evolution reaction[171] as well as CO_2 capture[172]. Perhaps the most straightforward yet also most promising function based on porous 2D polymers involves the chemical interaction of a target analyte with the pores producing an electrical or optical signal. Due to their unique electronic structure, π-conjugated 2D polymers should therefore be interesting candidates to develop materials for (bio)chemical detection with superior sensitivity combined with high selectivity. Considering the covalent 2D networks grown by on-surface polymerization discussed herein as building blocks (sheets) to construct 3D materials thereof, that is, covalent organic frameworks[28], many more applications in areas ranging from separation to catalysis as well as storage are imminent.

While most chemical applications eventually require large scales, the continuing miniaturization of electronic devices offers many opportunities for on-surface-grown molecular circuitry[173]. Charge transport through individual polymer chains and ribbons prepared in situ by on-surface polymerization has been realized and important design parameters for the construction of molecular wires continue to be derived[78,86,90,114,136,174]. This is a step further towards the realization of molecular logic gates by in situ assembly of a node from a core branching unit and defined oligomers as the leads to establish macroscopic contacts and probe different conjugation, thus conductance, paths[175]. In addition to transport properties, electroluminescence has also been observed in the case of single π-conjugated porphyrin–terthiophene copolymers, covalently assembled by on-surface polymerization and pulled into the STM junction[148,149]. Furthermore, by incorporating paramagnetic metal centres in monomers and branching units, spin wires, gates and tails have been covalently assembled and investigated as single-molecule logic devices[176,177]. The unique electronic properties of on-surface grown polymers have already been exploited in real device applications. For example, field-effect transistors with high on-current and high on–off ratio at room temperature have successfully been realized using high-quality GNRs prepared by on-surface synthesis[33,178], and further innovation can be expected in the field of electronic and optoelectronic devices.

The rise of on-surface synthesis and polymerization during the past decade has proven how fruitful the marriage of organic chemistry and surface science — two typically disjointed fields — can be. By combining key skills to design and make suitable molecular precursors on the one hand and to execute and analyse cutting-edge microscopic and spectroscopic experiments on the other hand, many more exciting discoveries are ahead.

Received: 16 February 2019; Accepted: 13 November 2019;
Published online: 29 January 2020

References

1. Ziegler, K. Folgen und Werdegang einer Erfindung (Nobel lecture). *Angew. Chem.* **76**, 545–553 (1964).
2. Binnig, G., Rohrer, H., Gerber, C. & Weibel, E. Tunneling through a controllable vacuum gap. *Appl. Phys. Lett.* **40**, 178–180 (1982).
3. Ertl, G. Reactions at surfaces: from atoms to complexity (Nobel lecture). *Angew. Chem. Int. Ed.* **47**, 3524–3535 (2008).
4. Theobald, J. A., Oxtoby, N. S., Phillips, M. A., Champness, N. R. & Beton, P. H. Controlling molecular deposition and layer structure with supramolecular surface assemblies. *Nature* **424**, 1029–1031 (2003).
5. Lin, N., Stepanow, S., Ruben, M. & Barth, J. V. Surface-confined supramolecular coordination chemistry. *Top. Curr. Chem.* **287**, 1–44 (2009).
6. Drexler, K. E. *Molecular Machinery and Manufacturing with Applications to Computation*. PhD thesis, Massachusetts Institute of Technology (1991).
7. Hla, S.-W., Bartels, L., Meyer, G. & Rieder, K.-H. Inducing all steps of a chemical reaction with the scanning tunneling microscope tip: towards single molecule engineering. *Phys. Rev. Lett.* **85**, 2777–2780 (2000).
8. Grill, L. et al. Nano-architectures by covalent assembly of molecular building blocks. *Nat. Nanotechnol.* **2**, 687–691 (2007).
9. Nacci, C., Hecht, S. & Grill, L. in *On-surface Synthesis* (ed. Gourdon, A.) 1–21 (Springer, 2016).
10. Gourdon, A. On-surface covalent coupling in ultrahigh vacuum. *Angew. Chem. Int. Ed.* **47**, 6950–6953 (2008).

11. Cai, J. et al. Atomically precise bottom-up fabrication of graphene nanoribbons. *Nature* **466**, 470–473 (2010).
12. Ruffieux, P. et al. On-surface synthesis of graphene nanoribbons with zigzag edge topology. *Nature* **531**, 489–492 (2016).
13. Boz, S., Stöhr, M., Soydaner, U. & Mayor, M. Protecting-group-controlled surface chemistry — organization and heat-induced coupling of 4,4-di(*tert*-butoxycarbonylamino)biphenyl on metal surfaces. *Angew. Chem. Int. Ed.* **48**, 3179–3183 (2009).
14. Sakamoto, J., van Heijst, J., Lukin, O. & Schlüter, A. D. Two-dimensional polymers: just a dream of synthetic chemists? *Angew. Chem. Int. Ed.* **48**, 1030–1069 (2009).
15. Kissel, P. et al. A two-dimensional polymer prepared by organic synthesis. *Nat. Chem.* **4**, 287–291 (2012).
16. Xi, M. & Bent, B. E. Iodobenzene on Cu(111): formation and coupling of adsorbed phenyl groups. *Surf. Sci.* **278**, 19–32 (1992).
17. Giessibl, F. J. Advances in atomic force microscopy. *Rev. Mod. Phys.* **75**, 949–983 (2003).
18. Gross, L., Mohn, F., Moll, N., Liljeroth, P. & Meyer, G. The chemical structure of a molecule resolved by atomic force microscopy. *Science* **325**, 1110–1114 (2009).
19. Gross, L. et al. Bond-order discrimination by atomic force microscopy. *Science* **337**, 1326–1329 (2012).
20. Pavlicek, N. et al. On-surface generation and imaging of arynes by atomic force microscopy. *Nat. Chem.* **7**, 623–628 (2015).
21. Mairena, A. et al. The fate of bromine after temperature-induced dehydrogenation of on-surface synthesized bisheptahelicene. *Chem. Sci.* **10**, 2998–3004 (2019).
22. Dienstmaier, J. F. et al. Synthesis of well-ordered COF monolayers: surface growth of nanocrystalline precursors versus direct on-surface polycondensation. *ACS Nano* **5**, 9737–9745 (2011).
23. Sakaguchi, H., Matsumura, H. & Gong, H. Electrochemical epitaxial polymerization of single-molecular wires. *Nat. Mater.* **3**, 551–557 (2004).
24. Colson, J. W. et al. Oriented 2D covalent organic framework thin films on single-layer graphene. *Science* **332**, 228–231 (2011).
25. Carothers, W. H. Polymerization. *Chem. Rev.* **8**, 353–426 (1931).
26. Szwarc, M. 'Living' polymers. *Nature* **178**, 1168–1169 (1956).
27. Lutz, J.-F., Lehn, J.-M., Meijer, E. W. & Matyjaszewski, K. From precision polymers to complex materials and systems. *Nat. Rev. Mater.* **1**, 16024 (2016).
28. Diercks, C. S. & Yaghi, O. M. The atom, the molecule, and the covalent organic framework. *Science* **355**, eaal1585 (2017).
29. Merrifield, R. B. Solid phase synthesis (Nobel lecture). *Angew. Chem. Int. Ed.* **24**, 799–892 (1985).
30. Matena, M., Riehm, T., Stöhr, M., Jung, T. A. & Gade, L. H. Transforming surface coordination polymers into covalent surface polymers: linked polycondensed aromatics through oligomerization of N-heterocyclic carbene intermediates. *Angew. Chem. Int. Ed.* **47**, 2414–2417 (2008).
31. Sun, Q. et al. On-surface formation of one-dimensional polyphenylene through Bergman cyclization. *J. Am. Chem. Soc.* **135**, 8448–8451 (2013).
32. Riss, A. et al. Local electronic and chemical structure of oligo-acetylene derivatives formed through radical cyclizations at a surface. *Nano Lett.* **14**, 2251–2255 (2014).
33. Sakaguchi, H., Song, S., Kojima, T. & Nakae, T. Homochiral polymerization-driven selective growth of graphene nanoribbons. *Nat. Chem.* **9**, 57–63 (2017).
34. Okawa, Y. & Aono, M. Nanoscale control of chain polymerization. *Nature* **409**, 683–684 (2001).
35. Okawa, Y. & Aono, M. Linear chain polymerization initiated by a scanning tunneling microscope tip at designated positions. *J. Chem. Phys.* **115**, 2317–2322 (2001).
36. Okawa, Y. et al. Chemical wiring and soldering toward all-molecule electronic circuitry. *J. Am. Chem. Soc.* **133**, 8227–8233 (2011).
37. Para, F. et al. Micrometre-long covalent organic fibres by photoinitiated chain-growth radical polymerization on an alkali-halide surface. *Nat. Chem.* **10**, 1112–1117 (2018).
38. Hodge, P. Entropically driven ring-opening polymerization of strainless organic macrocycles. *Chem. Rev.* **114**, 2278–2312 (2014).
39. Sassi, M., Oison, V., Debierre, J.-M. & Humbel, S. Modelling the two-dimensional polymerization of 1,4-benzene diboronic acid on a Ag surface. *ChemPhysChem* **10**, 2480–2485 (2009).
40. DeGreef, T. F. A. et al. Supramolecular polymerization. *Chem. Rev.* **109**, 5687–5754 (2009).
41. Björk, J. & Hanke, F. Towards design rules for covalent nanostructures on metal surfaces. *Chem. Eur. J.* **20**, 928–934 (2014).
42. Bieri, M. et al. Two-dimensional polymer formation on surfaces: insight into the roles of precursor mobility and reactivity. *J. Am. Chem. Soc.* **132**, 16669–16676 (2010).
43. DiGiovannantonio, M. et al. Mechanistic picture and kinetic analysis of surface-confined Ullmann polymerization. *J. Am. Chem. Soc.* **138**, 16696–16702 (2016).
44. Ferrighi, L. et al. Control of the intermolecular coupling of dibromotetracene on Cu(110) by the sequential activation of C–Br and C–H bonds. *Chem. Eur. J.* **21**, 5826–5835 (2015).
45. Cai, L. et al. Direct formation of C–C double-bonded structural motifs by on-surface dehalogenative homocoupling of *gem*-dibromomethyl molecules. *ACS Nano* **12**, 7959–7966 (2018).
46. Sun, Q. et al. Direct formation of C–C triple-bonded structural motifs by on-surface dehalogenative homocouplings of tribromomethyl-substituted arenes. *Angew. Chem. Int. Ed.* **57**, 4035–4038 (2018).
47. Ertl, G. Elementary steps in heterogeneous catalysis. *Angew. Chem. Int. Ed.* **29**, 1219–1227 (1990).
48. Weigelt, S. et al. Covalent interlinking of an aldehyde and an amine on an Au(111) surface in ultrahigh vacuum. *Angew. Chem. Int. Ed.* **46**, 9227–9230 (2007).
49. Lafferentz, L. et al. Controlling on-surface polymerization by hierarchical and substrate-directed growth. *Nat. Chem.* **4**, 215–220 (2012).
50. Veld, M. I., Iavicoli, P., Haq, S., Amabilino, D. B. & Raval, R. Unique intermolecular reaction of simple porphyrins at a metal surface gives covalent nanostructures. *Chem. Commun*. 1536–1538 (2008).
51. Lipton-Duffin, J. A., Ivasenko, O., Perepichka, D. F. & Rosei, F. Synthesis of polyphenylene molecular wires by surface-confined polymerization. *Small* **5**, 592–597 (2009).
52. Zwaneveld, N. A. A. et al. Organized formation of 2D extended covalent organic frameworks at surfaces. *J. Am. Chem. Soc.* **130**, 6678–6679 (2008).
53. Ourdjini, O. et al. Substrate-mediated ordering and defect analysis of a surface covalent organic framework. *Phys. Rev. B* **84**, 125421 (2011).
54. Gutzler, R. et al. Surface mediated synthesis of 2D covalent organic frameworks: 1,3,5-tris(4-bromophenyl)benzene on graphite(001), Cu(111), and Ag(110). *Chem. Commun*. 4456–4458 (2009).
55. Koch, M., Gille, M., Viertel, A., Hecht, S. & Grill, L. Substrate-controlled linking of molecular building blocks: Au(111) vs. Cu(111). *Surf. Sci.* **627**, 70–74 (2014).
56. Pham, T. A. et al. Comparing Ullmann coupling on noble metal surfaces: on-surface polymerization of 1,3,6,8-tetrabromopyrene on Cu(111) and Au(111). *Chem. Eur. J.* **22**, 5937–5944 (2016).
57. Simonov, K. A. et al. From graphene nanoribbons on Cu(111) to nanographene on Cu(110): critical role of substrate structure in the bottom-up fabrication strategy. *ACS Nano* **9**, 8997–9011 (2015).
58. Pinardi, A. L. et al. Tailored formation of N-doped nanoarchitectures by diffusion-controlled on-surface (cyclo)-dehydrogenation of heteroaromatics. *ACS Nano* **7**, 3676–3684 (2013).
59. Koch, M., Gille, M., Hecht, S. & Grill, L. Steering a cycloaddition reaction via the surface structure. *Surf. Sci.* **678**, 194–200 (2018).
60. Saywell, A., Schwarz, J., Hecht, S. & Grill, L. Polymerization on stepped surfaces: alignment of polymers and identification of catalytic sites. *Angew. Chem. Int. Ed.* **51**, 5096–5100 (2012).
61. Han, P. et al. Bottom-up graphene-nanoribbon fabrication reveals chiral edges and enantioselectivity. *ACS Nano* **8**, 9181–9187 (2014).
62. Simonov, K. A. et al. Comment on 'Bottom-up graphene-nanoribbon fabrication reveals chiral edges and enantioselectivity'. *ACS Nano* **9**, 3399–3403 (2015).
63. Han, P. et al. Reply to "Comment on 'Bottom-up graphene-nanoribbon fabrication reveals chiral edges and enantioselectivity'". *ACS Nano* **9**, 3404–3405 (2015).
64. Huang, H. et al. Spatially resolved electronic structure of precise armchair graphene nanoribbons. *Sci. Rep.* **2**, 983 (2012).
65. Sanchez-Sanchez, C. et al. Purely armchair or partially chiral: noncontact atomic force microscopy characterization of dibromo-bianthryl-based graphene nanoribbons grown on Cu(111). *ACS Nano* **10**, 8006–8011 (2016).
66. Schulz, F. et al. Precursor geometry determines the growth mechanism in graphene nanoribbons. *J. Phys. Chem. C* **121**, 2896–2904 (2017).
67. Villagomez, C. J., Sasaki, T., Tour, J. M. & Grill, L. Bottom-up assembly of molecular wagons on a surface. *J. Am. Chem. Soc.* **132**, 16848 (2010).
68. Bieri, M. et al. Surface-supported 2D heterotriangulene polymers. *Chem. Commun.* **47**, 10239–10241 (2011).
69. Bulou, H. & Massobrio, C. Mechanisms of exchange diffusion on fcc(111) transition metal surfaces. *Phys. Rev. B* **72**, 205427 (2005).
70. Wang, W., Shi, X., Wang, S., VanHove, M. A. & Lin, N. Single-molecule resolution of an organometallic intermediate in a surface-supported Ullmann coupling reaction. *J. Am. Chem. Soc.* **133**, 13264–13267 (2011).
71. Zint, S. et al. Imaging successive intermediate states of the on-surface Ullmann reaction on Cu(111): role of the metal coordination. *ACS Nano* **11**, 4183–4190 (2017).
72. Eder, G. et al. Solution preparation of two-dimensional covalently linked networks by polymerization of 1,3,5-tri(4-iodophenyl)benzene on Au(111). *ACS Nano* **7**, 3014–3021 (2013).
73. Adisoejoso, J. et al. A single-molecule-level mechanistic study of Pd-catalyzed and Cu-catalyzed homocoupling of aryl bromide on an Au(111) surface. *Chem. Eur. J.* **20**, 4111–4116 (2014).

74. Kittelmann, M. et al. On-surface covalent linking of organic building blocks on a bulk insulator. *ACS Nano* **5**, 8420–8425 (2011).
75. Kittelmann, M., Nimmrich, M., Lindner, R., Gourdon, A. & Kühnle, A. Sequential and site-specific on-surface synthesis on a bulk insulator. *ACS Nano* **7**, 5614–5620 (2013).
76. Repp, J., Meyer, G., Stojkovic, S. M., Gourdon, A. & Joachim, J. Molecules on insulating films: scanning-tunneling microscopy imaging of individual molecular orbitals. *Phys. Rev. Lett.* **94**, 026803 (2005).
77. Wang, S. et al. Giant edge state splitting at atomically precise graphene zigzag edges. *Nat. Commun.* **7**, 11507 (2016).
78. Jacobse, P. H., Mangnus, M. J. J., Zevenhuizen, S. J. M. & Swart, I. Mapping the conductance of electronically decoupled graphene nanoribbons. *ACS Nano* **12**, 7048–7056 (2018).
79. Bombis, C. et al. Single molecular wires connecting metallic and insulating surface areas. *Angew. Chem. Int. Ed.* **48**, 9966–9970 (2009).
80. Berner, S. et al. Boron nitride nanomesh: functionality from a corrugated monolayer. *Angew. Chem. Int. Ed.* **46**, 5115–5119 (2007).
81. Zhao, W., Dong, L., Huang, C., Win, Z. M. & Lin, N. Cu- and Pd-catalyzed Ullmann reaction on a hexagonal boron nitride layer. *Chem. Commun.* **52**, 13225–13228 (2016).
82. Berner, N. C. et al. Adsorption of 5,10,15,20-tetrakis(4-bromophenyl) porphyrin on germanium(001). *Phys. Status Solidi C* **9**, 1404–1407 (2012).
83. Olszowski, P. et al. Aryl halide C–C coupling on Ge(001):H surfaces. *J. Phys. Chem. C* **119**, 27478–27482 (2015).
84. Kolmer, M. et al. Polymerization of polyanthrylene on a titanium dioxide (011)-(2×1) surface. *Angew. Chem. Int. Ed.* **52**, 10300–10303 (2013).
85. Kolmer, M. et al. On-surface polymerization on a semiconducting oxide: aryl halide coupling controlled by surface hydroxyl groups on rutile TiO_2(011). *Chem. Commun.* **51**, 11276 (2015).
86. Koch, M., Ample, F., Joachim, C. & Grill, L. Voltage-dependent conductance of a single graphene nanoribbon. *Nat. Nanotechnol.* **7**, 713–717 (2012).
87. Koch, M. *Growth and Characterization of Single Molecular Wires on Metal Surfaces.* PhD thesis, Free University Berlin (2013).
88. Lipton-Duffin, J. A. et al. Step-by-step growth of epitaxially aligned polythiophene by surface-confined reaction. *Proc. Natl Acad. Sci. USA* **107**, 11200–11204 (2010).
89. Linden, S. et al. Electronic structure of spatially aligned graphene nanoribbons on Au(788). *Phys. Rev. Lett.* **108**, 216801 (2012).
90. Lafferentz, L. et al. Conductance of a single conjugated polymer as a continuous function of its length. *Science* **323**, 1193–1197 (2009).
91. Zhong, D. et al. Linear alkane polymerization on a gold surface. *Science* **334**, 213–216 (2011).
92. Cai, Z., She, L., Wu, L. & Zhong, D. On-surface synthesis of linear polyphenyl wires guided by surface steric effect. *J. Phys. Chem. C* **120**, 6619–6624 (2016).
93. Vasseur, G. et al. π band dispersion along conjugated organic nanowires synthesized on a metal oxide semiconductor. *J. Am. Chem. Soc.* **138**, 5685–5692 (2016).
94. Dai, J. et al. The role of the substrate structure in the on-surface synthesis of organometallic and covalent oligophenylene chains. *Phys. Chem. Chem. Phys* **18**, 20627–20634 (2016).
95. Fan, Q. et al. Surface-assisted organic synthesis of hyperbenzene nanotroughs. *Angew. Chem. Int. Ed.* **52**, 4668–4672 (2013).
96. Lin, T., Shang, X. S., Adisoejoso, J., Liu, P. N. & Lin, N. Steering on-surface polymerization with metal-directed template. *J. Am. Chem. Soc.* **135**, 3576–3582 (2013).
97. Otero, R. et al. Lock-and-key effect in the surface diffusion of large organic molecules probed by STM. *Nat. Mater.* **3**, 779 (2004).
98. Miura, A. et al. Light- and STM tip-induced formation of one-dimensional and two-dimensional organic nanostructures. *Langmuir* **19**, 6474–6482 (2003).
99. Flory, P. J. *Principles of Polymer Chemistry* (Cornell Univ. Press, 1953).
100. Adisoejoso, J., Li, Y., Liu, J., Liu, P. N. & Lin, N. Two-dimensional metallo-supramolecular polymerization: toward size-controlled multi-strand polymers. *J. Am. Chem. Soc.* **134**, 18526–18529 (2012).
101. Held, P. A., Fuchs, H. & Studer, A. Covalent-bond formation via on-surface chemistry. *Chem. Eur. J.* **23**, 5874–5892 (2017).
102. Xi, M. & Bent, B. E. Mechanisms of the Ullmann coupling reaction in adsorbed monolayers. *J. Am. Chem. Soc.* **115**, 7426–7433 (1993).
103. Lackinger, M. Surface-assisted Ullmann coupling. *Chem. Commun.* **53**, 7872–7885 (2017).
104. McCarty, G. S. & Weiss, P. S. Formation and manipulation of protopolymer chains. *J. Am. Chem. Soc.* **126**, 16772–16776 (2004).
105. Klappenberger, F. et al. On-surface synthesis of carbon-based scaffolds and nanomaterials using terminal alkynes. *Acc. Chem. Res.* **48**, 2140–2150 (2015).
106. Marele, A. C. et al. Formation of a surface covalent organic framework based on polyester condensation. *Chem. Commun.* **48**, 6779–6781 (2012).
107. Treier, M., Richardson, N. V. & Fasel, R. Fabrication of surface-supported low-dimensional polyimide networks. *J. Am. Chem. Soc.* **130**, 14054–14055 (2008).
108. Weigelt, S. et al. Surface synthesis of 2D branched polymer nanostructures. *Angew. Chem. Int. Ed.* **47**, 4406–4410 (2008).
109. Jiang, L. et al. Synthesis of pyrene-fused pyrazaacenes on metal surfaces: toward one-dimensional conjugated nanostructures. *ACS Nano* **10**, 1033–1041 (2016).
110. Schlögl, S., Sirtl, T., Eichhorn, J., Heckl, W. M. & Lackinger, M. Synthesis of two-dimensional phenylene-boroxine networks through in vacuo condensation and on-surface radical addition. *Chem. Commun.* **47**, 12355–12357 (2011).
111. Schuurmans, N. et al. Design and STM investigation of intramolecular folding in self-assembled monolayers on the surface. *J. Am. Chem. Soc.* **126**, 13884–13885 (2004).
112. Schmitz, C. H., Ikonomov, J. & Sokolowski, M. Two-dimensional ordering of poly(*p*-phenylene-terephthalamide) on the Ag(111) surface investigated by scanning tunneling microscopy. *J. Phys. Chem. C* **113**, 11984–11987 (2009).
113. Jacobse, P. H., vandenHoogenband, A., Moret, M.-E., Gebbink, R. J. M. K. & Swart, I. Aryl radical geometry determines nanographene formation on Au(111). *Angew. Chem. Int. Ed.* **55**, 13052–13055 (2016).
114. Jacobse, P. H. et al. Electronic components embedded in a single graphene nanoribbon. *Nat. Commun.* **8**, 119 (2017).
115. Zhang, H. M. et al. On-surface synthesis of rylene-type graphene nanoribbons. *J. Am. Chem. Soc.* **137**, 4022–4025 (2015).
116. Chen, Y.-C. et al. Tuning the band gap of graphene nanoribbons sythesized from molecular precursors. *ACS Nano* **7**, 6123–6128 (2013).
117. Nguyen, G. D. et al. Bottom-up synthesis of $N = 13$ sulfur-doped graphene nanoribbons. *J. Phys. Chem. C* **120**, 2684–2687 (2016).
118. Bronner, C. et al. Aligning the band gap of graphene nanoribbons by monomer doping. *Angew. Chem. Int. Ed.* **52**, 4422–4425 (2013).
119. Cai, J. et al. Graphene nanoribbon heterojunctions. *Nat. Nanotechnol.* **9**, 896–900 (2014).
120. Kawai, S. et al. Atomically controlled substitutional boron-doping of graphene nanoribbons. *Nat. Commun.* **6**, 8098 (2015).
121. Cloke, R. R. et al. Site-specific substitutional boron doping of semiconducting armchair graphene nanoribbons. *J. Am. Chem. Soc.* **137**, 8872–8875 (2015).
122. Krasnikov, S. A. et al. Formation of extended covalently bonded Ni porphyrin networks on the Au(111) surface. *Nano Res.* **4**, 376–384 (2011).
123. Koudia, M. & Abel, M. Step-by-step on-surface synthesis: from manganese phthalocyanines to their polymeric form. *Chem. Commun.* **59**, 8565–8567 (2014).
124. Bieri, M. et al. Porous graphenes: two-dimensional polymer synthesis with atomic precision. *Chem. Commun.* **2009**, 6919–6921 (2009).
125. Eichhorn, J. et al. On-surface Ullmann coupling: the influence of kinetic reaction parameters on the morphology and quality of covalent networks. *ACS Nano* **8**, 7880–7889 (2014).
126. Ma, C. et al. Seamless staircase electrical contact to semiconducting graphene nanoribbons. *Nano Lett.* **17**, 6241–6247 (2017).
127. Müllegger, S. & Winkler, A. Dehydrogenation of oligo-phenylenes on gold surfaces. *Surf. Sci.* **600**, 3982–3986 (2006).
128. Moreno, C. et al. Bottom-up synthesis of multifunctional nanoporous graphene. *Science* **360**, 199–203 (2018).
129. Guan, C.-Z., Wang, D. & Wan, L.-J. Construction and repair of highly ordered 2D covalent networks by chemical equilibrium regulation. *Chem. Commun.* **48**, 2943–2945 (2012).
130. Dienstmaier, J. F. et al. Isoreticular two-dimensional covalent organic frameworks synthesized by on-surface condensation of diboronic acids. *ACS Nano* **6**, 7234–7242 (2012).
131. Spitzer, S. et al. Solvent-free on-surface synthesis of boroxine COF monolayers. *Chem. Commun.* **53**, 5147–5150 (2017).
132. Arado, O. D. et al. On-surface azide-alkyne cycloaddition on Au(111). *ACS Nano* **7**, 8509–8515 (2013).
133. Cote, A. P. et al. Porous, crystalline, covalent organic frameworks. *Science* **310**, 1166–1170 (2005).
134. Gröning, O. et al. Engineering of robust topological quantum phases in graphene nanoribbons. *Nature* **560**, 209–213 (2018).
135. Rizzo, D. J. et al. Topological band engineering of graphene nanoribbons. *Nature* **560**, 204–208 (2018).
136. Nacci, C. et al. Conductance of a single flexible molecular wire composed of alternating donor and acceptor units. *Nat. Commun.* **6**, 7397 (2015).
137. Sakaguchi, H., Matsumura, H., Gong, H. & Abouelwafa, A. M. Direct visualization of the formation of single-molecule conjugated copolymers. *Science* **310**, 1002–1006 (2005).
138. Clair, S., Ourdjini, O., Abel, M. & Porte, L. Tip- or electron beam-induced surface polymerization. *Chem. Commun.* **47**, 8028–8030 (2011).
139. Deshpande, A. et al. Self-assembly and photopolymerization of sub-2 nm one-dimensional organic nanostructures on graphene. *J. Am. Chem. Soc.* **134**, 16759–16764 (2012).

140. Shen, Q. et al. Self-assembled two-dimensional nanoporous molecular arrays and photoinduced polymerization of 4-bromo-4′-hydroxybiphenyl on Ag(111). *J. Chem. Phys.* **142**, 101902 (2015).
141. Ho, W. Inducing and viewing bond selected chemistry with tunneling electrons. *Acc. Chem. Res.* **31**, 567–573 (1998).
142. Hla, S.-W., Meyer, G. & Rieder, K.-H. Inducing single-molecule chemical reactions with a UHV-STM: a new dimension for nano-science and technology. *ChemPhysChem* **2**, 361–366 (2001).
143. Hahn, J. R. & Ho, W. Oxidation of a single carbon monoxide molecule manipulated and induced with a scanning tunneling microscope. *Phys. Rev. Lett.* **87**, 166102 (2001).
144. Anggara, K., Leung, L., Timm, M. J., Hu, Z. & Polanyi, J. C. Approaching the forbidden fruit of reaction dynamics: aiming reagent at selected impact parameters. *Sci. Adv.* **4**, eaau2821 (2018).
145. Wegner, G. Topochemical polymerization of monomers with conjugated triple bonds. *Makromol. Chem.* **154**, 35–48 (1972).
146. Pavlicek, N. et al. Polyyne formation via skeletal rearrangement induced by atomic manipulation. *Nat. Chem.* **10**, 853–858 (2018).
147. Patera, L. L. et al. Real-time imaging of adatom-promoted graphene growth on nickel. *Science* **359**, 1243–1246 (2018).
148. Chong, M. C. et al. Narrow-line single-molecule transducer between electronic circuits and surface plasmons. *Phys. Rev. Lett.* **116**, 036802 (2016).
149. Chong, M. C. et al. Ordinary and hot electroluminescence from single-molecule devices: controlling the emission color by chemical engineering. *Nano Lett.* **16**, 6480–6484 (2016).
150. Kawai, S. et al. Quantifying the atomic-level mechanics of single long physisorbed molecular chains. *Proc. Natl Acad. Sci. USA* **111**, 3968–3972 (2014).
151. Kawai, S. et al. Superlubricity of graphene nanoribbons on gold surfaces. *Science* **351**, 957–961 (2016).
152. Koch, M. et al. How structural defects affect the mechanical and electrical properties of single molecular wires. *Phys. Rev. Lett.* **121**, 047701 (2018).
153. Pavlicek, N. & Gross, L. Generation, manipulation and characterization of molecules by atomic force microscopy. *Nat. Rev. Chem.* **1**, 0005 (2017).
154. Wang, S., Wang, W. & Lin, N. Resolving band-structure evolution and defect-induced states of single conjugated oligomers by scanning tunneling microscopy and tight-binding calculations. *Phys. Rev. Lett.* **106**, 206803 (2011).
155. Vasseur, G. et al. Quasi one-dimensional band dispersion and surface metallization in long-range ordered polymeric wires. *Nat. Commun.* **7**, 10235 (2016).
156. Morchutt, C. et al. Interplay of chemical and electronic structure on the single-molecule level in 2D polymerization. *ACS Nano* **10**, 11511–11518 (2016).
157. Gutzler, R. & Perepichka, D. F. π–electron conjugation in two dimensions. *J. Am. Chem. Soc.* **135**, 16585–16594 (2013).
158. Cardenas, L. et al. Synthesis and electronic structure of a two dimensional π-conjugated polythiophene. *Chem. Sci.* **4**, 3263–3268 (2013).
159. Gutzler, R. Band-structure engineering in conjugated 2D polymers. *Phys. Chem. Chem. Phys* **18**, 29092–29100 (2016).
160. Chen, Z. et al. A heterogeneous single-atom palladium catalyst surpassing homogeneous systems for Suzuki coupling. *Nat. Nanotechnol.* **13**, 702–707 (2018).
161. Lopinski, G. P., Wayner, D. D. M. & Wolkow, R. A. Self-directed growth of molecular nanostructures on silicon. *Nature* **406**, 48–51 (2000).
162. Maksymovych, P., Sorescu, D. C., Jordan, K. D. & Yates, J. T. Collective reactivity of molecular chains self-assembled on a surface. *Science* **322**, 1664–1667 (2008).
163. Haq, S. et al. Versatile bottom-up construction of diverse macromolecules on a surface observed by scanning tunneling microscopy. *ACS Nano* **8**, 8856–8870 (2014).
164. Liu, J. & Wöll, C. Surface-supported metal-organic framework thin films: fabrication methods, applications, and challenges. *Chem. Soc. Rev.* **46**, 5730–5770 (2017).
165. Wintterlin, J. & Bocquet, M.-L. Graphene on metal surfaces. *Surf. Sci.* **603**, 1841–1852 (2009).
166. Nagashima, A., Tejima, N., Gamou, Y., Kawai, T. & Oshima, C. Electronic dispersion relations of monolayer hexagonal boron nitride formed on the Ni(111) surface. *Phys. Rev. B* **51**, 4606–4613 (1995).
167. Fairbrother, A. et al. High vacuum synthesis and ambient stability of bottom-up graphene nanoribbons. *Nanoscale* **9**, 2785–2792 (2017).
168. Chen, Z. P. et al. Synthesis of graphene nanoribbons by ambient-pressure chemical vapor deposition and device integration. *J. Am. Chem. Soc.* **138**, 15488–15496 (2016).
169. Deng, D. et al. Catalysis with two-dimensional materials and their heterostructures. *Nat. Nanotechnol.* **11**, 218–230 (2016).
170. Gutzler, R., Stepanow, S., Grumelli, D., Lingenfelder, M. & Kern, K. Mimicking enzymatic active sites on surfaces for energy conversion chemistry. *Acc. Chem. Res.* **48**, 2132–2139 (2015).
171. Wurster, B., Grumelli, D., Hötger, D., Gutzler, R. & Kern, K. Driving the oxygen evolution reaction by nonlinear cooperativity in bimetallic coordination catalysts. *J. Am. Chem. Soc.* **138**, 3623–3626 (2016).
172. Feng, M., Sun, H., Zhao, J. & Petek, H. Self-catalyzed carbon dioxide adsorption by metal-organic chains on gold surfaces. *ACS Nano* **8**, 8644–8652 (2014).
173. Aviram, A. & Ratner, M. Molecular rectifiers. *Chem. Phys. Lett.* **29**, 277–283 (1974).
174. Kuang, G. et al. Negative differential conductance in polyporphyrin oligomers with nonlinear backbones. *J. Am. Chem. Soc.* **140**, 570–573 (2018).
175. Nacci, C., Viertel, A., Hecht, S. & Grill, L. Covalent assembly and characterization of nonsymmetrical single-molecule nodes. *Angew. Chem. Int. Ed.* **55**, 13724–13728 (2016).
176. DiLullo, A. et al. Molecular Kondo chain. *Nano Lett.* **12**, 3174–3179 (2012).
177. Bazarnik, M. et al. Toward tailored all-spin molecular device. *Nano Lett.* **16**, 577–582 (2016).
178. Llinas, J. P. et al. Short-channel field effect transistors with 9-atom and 13-atom wide graphene nanoribbons. *Nat. Commun.* **8**, 633 (2017).
179. Kawai, S. et al. Diacetylene linked anthracene oligomers synthesized by one-shot homocoupling of trimethylsilyl on Cu(111). *ACS Nano* **12**, 8791–8797 (2018).

Acknowledgements

We are indebted to our co-workers for their valuable contributions to the field over the years that have been generously supported by the European Union (via integrated projects 'pico inside', 'ARTIST' and 'AtMol') as well as the German Research Foundation (DFG via GR 2697/1-1 as well as SFB 658 and SFB 951). This Review Article is dedicated to the memory of Karl-Heinz Rieder.

Author contributions

L.G. and S.H. contributed equally to the manuscript.

Competing interests

The authors declare no competing interests.

Additional information

Correspondence should be addressed to L.G. or S.H.

Reprints and permissions information is available at www.nature.com/reprints.

Publisher's note Springer Nature remains neutral with regard to jurisdictional claims in published maps and institutional affiliations.